THE INTERACTING EFFECTS OF LOCAL CONDITIONS AND SAHARAN DUST DEPOSITION ON *VIBRIO* POPULATION DYNAMICS IN NEARSHORE COASTAL WATERS

by

NATHAN WILLIAM GREENSLIT

(Under the Direction of Erin Lipp)

ABSTRACT

Episodic plumes of Saharan dust travel across the Atlantic to be deposited in the surface waters of the Gulf of Mexico. Dust aerosols have been shown to serve as a significant source of nutrients that can potentially facilitate the development of microbial blooms (including *Vibrio*) in offshore environments. However, the potential effect in more dynamic inland coastal waters is not known. This study aimed to quantify *Vibrio* population dynamics in response to dust events in regions where environmental parameters are more variable, and human risk of exposure is higher. Samples were collected during a Saharan dust event in summer 2022. During dust days, total *Vibrio* concentrations increased significantly but varied by site and the interacting effects of salinity and nutrient levels. This study provides an increased understanding of the conditions that can elicit blooms of *Vibrio* in coastal and inland regions where risk of human exposure is more likely.

INDEX WORDS: Saharan dust, Time series, Corpus Christi, Texas, Coastal, Inland, Vibrionaceae, *Vibrio*, Blooms, Nutrients, quantitative PCR

THE INTERACTING EFFECTS OF LOCAL CONDITIONS AND SAHARAN DUST DEPOSITION ON *VIBRIO* POPULATION DYNAMICS IN NEARSHORE COASTAL WATERS

by

NATHAN WILLIAM GREENSLIT

B.S., Clemson University, 2020

A Thesis Submitted to the Graduate Faculty of The University of Georgia in Partial Fulfillment of the Requirements for the Degree

MASTER OF SCIENCE

ATHENS, GEORGIA

2023

© 2023

Nathan William Greenslit

All Rights Reserved

THE INTERACTING EFFECTS OF LOCAL CONDITIONS AND SAHARAN DUST DEPOSITION ON *VIBRIO* POPULATION DYNAMICS IN NEARSHORE COASTAL WATERS

by

NATHAN WILLIAM GREENSLIT

Major Professor:	Erin K. Lipp
Committee:	Michael S. Wetz
	Patricia L. Yager
	James W. Porter

Electronic Version Approved:

Ron Walcott
Vice Provost for Graduate Education and Dean of the Graduate School
The University of Georgia
December 2023

ACKNOWLEDGEMENTS

Immense thanks to my advisor Dr. Erin Lipp for her mentorship, support, and kindness. She introduced me to the wonderful world of microbiology, and it has been such an amazing, inspirational, and educational experience getting to working with her. Thank you to my committee, Drs. Michael Wetz, James Porter, and Patricia Yager, and my faculty mentor Dr. Christof Meile, for your enthusiasm and guidance during my time as a graduate student. A huge thank you to the amazing team at Texas A&M Corpus Christi for welcoming me into the adventure of field work. Thank you to the past and present Lipp Lab members, who showed me the way in a microbiology lab and were a constant source of knowledge, humor, and shenanigans. Special love to all of my friends in the Marine Sciences and Environmental Health Science departments. Thank you to my great Aunt Jill, for making me feel at home in Athens and for our great dinners at Longhorn Steakhouse. Thank you to my mother and father for your support and love throughout my life, always inspiring me to pursue adventure and knowledge and thank you to my sisters, Katie, Lily, and Faya. I am also thankful for my loving cat Jiji. Lastly, thank you to my fiancé Olivia, for supporting me no matter what and being a source of comfort and counsel.

TABLE OF CONTENTS

Page

LIST OF TABLES

Page

CHAPTERS

LIST OF FIGURES

Page

CHAPTERS

CHAPTER 1

INTRODUCTION AND LITERATURE REVIEW

Introduction

Vibrio are gram-negative, rod-shaped, heterotrophic bacteria that belong to the class γ-proteobacteria and family *Vibrionaceae* and are natural constituents of marine and brackish waters. A subset of species within *Vibrionaceae* are known to be associated with human disease, and in tandem with rising sea surface temperatures, cases have been increasing globally and expanding geographically. Surveillance data indicates that in the U.S. alone, *Vibrio* related illnesses have more than doubled since 1997 (CDC, 2023; Newton et al., 2012). Illnesses can be induced through either a dermal route (e.g. wound exposure to seawater) or through an oral route such as the ingestion of contaminated seafood (e.g. oysters) or water. Symptoms of infection can range from mild and self-limiting gastroenteritis, ear and wound infections, to fatal cases of necrotizing fasciitis and septicemia (Baker-Austin et al., 2018). *Vibrio* are considered conditionally rare, as they typically make up <1% of the bacterioplankton community, but under the right conditions they can quickly make up a larger portion of the microbial community. Previous work has shown increases in *Vibrio* abundances following nutrient pulse events from phytoplankton blooms (Gilbert et al., 2012; Greenfield et al., 2017) and heat waves (Baker-Austin et al., 2016), with recent evidence pointing to blooms following Saharan dust deposition (Borchardt et al., 2020; Westrich et al., 2016, 2018). Blooms of

potentially pathogenic bacteria, including *Vibrio* has the potential to pose a significant health risk to the public, as risk of exposure is heightened during these periods. Therefore, it becomes vital to understand how short-term environmental fluctuations may elicit increases in *Vibrio* abundance, and how these blooms may impact human health.

Vibrio **Epidemiology**

The genus *Vibrio* is comprised of over 100 species, 12 of which are known to be pathogenic to humans. Any *Vibrionaceae* infections are required to be reported to the CDC, as any species within that family have the potential to be pathogenic. Infections primarily occur through either an oral route via the consumption of raw or uncooked seafood (e.g. oysters) and contaminated drinking water, or through wound exposure. Symptoms of infection include mild and self-limiting gastroenteritis, diarrhea, nausea, wound and ear infections, and in some extreme cases necrotizing fasciitis and septicemia (Baker-Austin et al., 2018). The global case incidence of *Vibrio* infections is not well understood due to limitations in current surveillance systems and a high prevalence of underreporting, as *Vibrio*-related illnesses often result in cases of self-limiting symptoms. In the United States however, infections have been reported to the Cholera and Other *Vibrio* Illness Surveillance (COVIS) system since 1988, with an estimated 80,000 illnesses and 100 deaths each year. *Vibrio* infections typically have a summer seasonality with higher case counts between May and October (CDC, 2023) (Figure 1.1), and infections can be broken into two classifications: cholera, and non-cholera vibriosis, with four species globally dominating infection cases in humans: *V. alginolyticus*, *V. cholerae*, *V. parahaemolyticus*, and *V. vulnificus* (CDC, 2023).

V. cholerae is the causative agent of cholera, an acute enteric diarrheal disease that is of public health concern due to its high mortality rate. This bacterium is endemic to Southern Asia, parts of Africa and Latin America, and will often have seasonal outbreaks associated with poverty and poor sanitation. *V. cholera* is one of the most well-studied *Vibrio* bacteria, as there are an estimated 1.3 to 4.0 million cholera cases with approximately 21,000 to 143,000 deaths each year globally (World Health Organization, 2016). There have been 6 concluded pandemics since 1817, with the current 7th pandemic beginning in 1961 (Hu et al., 2016). These pandemics are driven by the O139 and O1 serotypes, which are classified based on the chemical composition of the O-antigen. Infections due to this bacterium are a result of the ingestion of contaminated drinking water or food followed by the production of cholera enterotoxin. The secretion of this toxin leads to mass ion and water transport by the intestinal epithelial cells and results in the characteristic watery-stool, further dispersing the bacterium (Maheshwari et al., 2011). While not as well studied, non-O139 and O1 serotype infections can result in mild cases of gastroenteritis and wound and ear infections (Deshayes et al., 2015).

V. vulnificus is responsible for approximately 95% of seafood related deaths and has an estimated 33% mortality rate in the United States alone (Baker-Austin & Oliver, 2018; Heng et al., 2017). Infection is primarily associated with men between the years of 45-60 with underlying risk factors including liver cirrhosis, diabetes, and immunodeficiency (Horseman & Surani, 2011). Less severe symptoms of infection include nausea, diarrhea, fever, and vomiting and although not as common, more extreme infections result in necrotizing fasciitis and septicemia, where case fatality rates are greater than 50% and about 15% respectively (Bross et al., 2007). Each year, there are

approximately 150-200 reported cases of infection, with approximately 1 in 5 people dying from infection (CDC Health Alert Network, 2023). This pathogen is commonly found in brackish waters with salinities ranging from 2-25 and warm waters exceeding 18°C and thus infection risks are higher in the warm summer months between May and October. The primary modes of infection are through the consumption of raw shellfish and environmental exposure to contaminated drinking water (Baker-Austin et al., 2018; Baker-Austin & Oliver, 2018; Coerdt & Khachemoune, 2021; Heng et al., 2017).

V. parahaemolyticus is the predominant bacterium that is associated with seafood (particularly oysters) induced food poisoning, resulting in acute gastroenteritis, wound infections, and in extreme cases septicemia (Baker-Austin et al., 2017; Daniels et al., 2000). An estimated 45,000 cases occur in the United States each year (CDC, 2019), but this value is likely underestimated, as many cases of infection are self-limiting and thus are not reported.

V. alginolyticus is a human pathogen that primarily results in wound and ear infections, gastroenteritis, and sepsis. Ear infections have been found to be predominant in children less than 5 years of age while lower extremity infections were more common in adults (Slifka et al., 2017). The past few decades have seen a dramatic increase of vibriosis case-incidence (Newton et al., 2012), with *V. alginolyticus* progressing from the third to the second most common in 2007 (CDC, 2023). As opposed to the other prominent *Vibrio* pathogens, *V. alginolyticus* is primarily transmitted through water, where infections can be induced through open wound exposure, thus a majority of infections occur in coastal regions.

A smaller subset of *Vibrio* species are associated with illnesses in marine organisms that are important for aquaculture and ecosystem stability. For example, *Vibrio* species have been shown to induce coral bleaching and tissue loss at elevated temperatures (*V. coralliilyticus*, *V. shiloi*, *V. alginolyticus*) and may play an opportunistic role in stony coral tissue loss disease (*V. coralliilyticus*) (Ben-Haim, Zicherman-Keren, et al., 2003; Ben-Haim & Rosenberg, 2002; Munn, 2015; Ushijima et al., 2020a). Several species of the *Vibrionaceae* family have been associated with outbreaks in aquaculture settings, causing mass mortality events in important fish species such as groupers, flounder, snappers, and seabreams, among others (*V. alginolyticus*, *V. vulnificus*, *V. parahaemolyticus*, *V. anguillarum*) (Ina-Salwany et al., 2019). Other species have been shown to induce mortality in penaeid shrimp (*V. parahaemolyticus*) as well as shellfish such as oysters (*V. coralliilyticus*) (Richards et al., 2015; Schryver et al., 2014; Tran et al., 2013).

Vibrio Ecology

Vibrio are heterotrophic bacteria that are ubiquitous in marine settings, ranging from coastal, pelagic, estuarine, brackish, and to some extent freshwater environments (Takemura et al., 2014). *Vibrio* can be free-living in the water column, particle associated, associated with a variety of organisms (plants, plankton, invertebrates), and in some cases exhibit symbiosis with marine organisms (Takemura et al., 2014). Close associations with plankton have been documented as they have the potential to serve as a nutrient-rich reservoir that can function as a source of growth for heterotrophic bacteria. The arthropod exoskeletons of zooplankton serve as a primary source of chitin, supplying important nutrients like nitrogen and carbon (Aunkham et al., 2018; Turner et al., 2009).

Vibrio have also been found to be in close association with various species of phytoplankton (diatoms, dinoflagellates, raphidophytes) as they excrete high amounts of fixed carbon through passive leakage or senescence that *Vibrio* species can utilize as a growth source (Asplund et al., 2011; Greenfield et al., 2017; Main et al., 2015).

Of the environmental correlates that drive *Vibrio* presence and abundance, temperature and salinity are the most prominent. Broadly, *Vibrio* can be found in higher abundances in warm (>15°C) waters with moderate salinities waters (~25) with highest abundances in the summer months (Froelich & Daines, 2020), however when it comes to specific species, physiochemical tolerances can vary, with some species preferring lower salinities (*V. mimicus, V. vulnificus*, *V. cholerae*), and others having a much broader environmental range (*V. alginolyticus, V. parahaemolyticus*) (Böer et al., 2013; Sampaio et al., 2022). While temperature, and to some degree salinity are the dominant environmental variables that explain *Vibrio* abundance and distribution, other biotic and abiotic components have been found to play a role as well. For example, *V. cholerae* has been found to be closely associated with zooplankton (e.g. copepods) (Pruzzo et al., 2008). *E. coli* and total coliforms have been observed to be positively correlated with *V. cholerae* and *V. parahaemolyticus* abundances, while these in addition to total bacteria have been identified as biotic correlates of *V. vulnificus*, though this may be a result of a large response to anthropogenic input of nutrients (e.g. wastewater discharge) (Blackwell & Oliver, 2008; Randa et al., 2004; Takemura et al., 2014). Other environmental factors such as nitrogen, phosphorous, dissolved oxygen, and dissolved organic carbon (DOC) have also been found to be highly associated with *Vibrio* abundance.

As obligate heterotrophs, *Vibrio* rely on various forms of organic matter as a carbon source. In general, most species are capable of utilizing over 40 different compounds of carbon as an energy source. These include polysaccharides such as chitin which are associated with zooplankton exoskeletons and alginate, which comprises brown algae cell walls (Zhang et al., 2018). Through both respiratory and fermentative respiration, *Vibrio* can transform the organic carbon into cell material and waste products including organic acids, alcohols and in some species H_2 (Thompson & Polz, 2006). *Vibrio* predation via protist grazing or viral lysis plays an important role in reintroducing the acquired carbon back into the environment, that can be further used as a nutrient source for subsequent populations (Kauffman et al., 2018; Zhang et al., 2018).

While ubiquitous in marine environments, *Vibrio* are characterized as conditionally rare, as they make up <1% of the bacterioplankton community (Thompson et al., 2004). Recent evidence has shown that under specific abiotic and biotic conditions, *Vibrio* abundances can rapidly increase resulting in blooms. Characterized as oppurtunitrophs, *Vibrio* have multiple advantages that allow them to gain the upper hand when responding to any newly introduced substrate or nutrients. *Vibrio* are among the fastest growing bacteria, with one species having a doubling time <10 minutes (Eagon, 1962). Their large genomic repertoire (consisting of two circular chromosomes and multiple copies of the 16S ribosomal RNA gene) that likely resulted from horizontal gene transfer, provides versatility in competing for resources in a broad range of biological niches (Jensen et al., 2009; Okada et al., 2005). Additionally, *Vibrio* exhibit efficient chemotactic motility, with the ability to rapidly respond to pulses of nutrients (Ringgaard et al., 2018). Among bacteria, *Vibrio* can maintain a competitive advantage for limiting

micronutrients like Fe through the utilization Fe-chelating siderophore complexes that allow for rapid uptake into the cell (Payne et al., 2016). Rapid increases in *Vibrio* abundance and case incidence have previously been documented following environmental fluctuations such as increases in DOM from harmful algal blooms, heat waves, and hurricanes (Baker-Austin et al., 2016; Greenfield et al., 2017; Sodders et al., 2023), with recent evidence pointing towards *Vibrio* blooms following Saharan dust deposition events (Borchardt et al., 2020; Westrich et al., 2016, 2018).

Saharan Dust Events

The Saharan desert is a major source of atmospheric dust, eliciting an estimated 800 Tg yr^{-1} into the atmosphere (Prospero et al., 2014). These dust aerosols can be transported northward across the Mediterranean to Europe, easterly to regions in the Middle East, with a majority being transported westward across the Atlantic to be deposited in the surface waters of the mid-Atlantic, Caribbean, and Gulf of Mexico (d'Almeida, 1986; Goudie & Middleton, 2001; Prospero, 1996). Dust settling typically occurs through dry or wet (precipitation) deposition resulting in hazy skies, bright orange sunsets, and rain events termed "blood rains" or "red rains". These dust events are highly episodic, occurring 3-4 times each year typically between May and October, lasting 3-5 days each. Dust events are typically tracked in one of four ways. Dust source areas can be identified from the specific chemical and mineral composition of the aerosols, satellite remote sensing techniques utilizing the UV and infrared radiative signature of dust to identify airborne dust aerosols, horizontal visibility can be used to determine local visibility, and Lagrangian back-track trajectories are commonly used to link dust sources to remote samples (Schepanski et al., 2012). Of the different methods, satellite remote

sensing is most common due to its spatiotemporal range and aerosols can be quantified using an aerosol optical thickness (AOT) index.

A wide diversity of microorganisms have been found to be associated with Saharan dust particles. This consists a variety of opportunistic bacterial pathogens (including species of *Staphylococcus* and *Bacillus*), fungal species (*Aspergillus* and *Cladosporium*), and virus-like particles (Griffin et al., 2001; Kellogg et al., 2004; Ramírez-Camejo et al., 2022). Deposition of potentially pathogenic microorganisms has the potential to pose a risk to the public health. Additionally, due to their small particle size ($PM_{2.5-10}$) dust particles can bypass the cilia and mucus barriers in the nose and throat and can penetrate the lungs resulting in respiratory illnesses including asthma, pneumonia, and tracheitis as well as cardiovascular disorders such as stroke, heart failure, and myocardial infarction (Akhtar, 2020).

Additionally, Saharan dust provides large quantities of nutrients that are essential for microbial growth. These aerosols consist of nutritive species including NO_3^-, PO_4^{3-}, K^+, NH_4^+ and Fe_2O_3 (Goudie & Middleton, 2001; Talbot et al., 1986a; Zhu et al., 1997). As dust is carried across the Atlantic it undergoes chemical and physical transformations including solar radiation, weathering, and gravitational sorting (Shi et al., 2011; van der Does et al., 2016). These atmospheric processes have been suggested to increase the solubility, and thus bioavailability, of dust-derived nutrients like Fe (Hand et al., 2004; Mahowald et al., 2005). Deposition of dust-derived bioavailable nutrients in otherwise nutrient limited settings can lead to the fertilization of downwind terrestrial and marine ecosystems. The Amazon Basin for example is typically limited by phosphorous, but is balanced by dust input sourced from the Bodélé Depression with an estimate 0.12 Tg of

phosphorous exported each year (Bristow et al., 2010; Koren et al., 2006). In marine systems, Saharan dust deposition has shown to result in the stimulation of *Trichodesmium* and subsequent blooms of harmful algal species *K. brevis* in the Gulf of Mexico (Lenes et al., 2008) and the West Florida Shelf (Walsh & Steidinger, 2001), and increases in abundance of *Synechococcus* in the Mediterranean Sea (Herut et al., 2005), with emerging evidence showing that heterotrophic bacteria, such as *Vibrio* are responding to the episodic influx of limiting resources and substrate, resulting in blooms of bacteria that are associated with disease (Borchardt et al., 2020; Westrich et al., 2016, 2018).

The Relationship between *Vibrio* and Dust

Previous work has characterized *Vibrio* blooms in response to Saharan dust input in the oligotrophic setting of the Caribbean and subtropical Atlantic (Barbados and Florida Keys, respectively), with surface water concentrations of total *Vibrio* increasing by five to thirty times that found during non-dust conditions and returning to baseline levels within 24-48 hours (Figure 1.2). *Vibrio* composition within the larger microbial community also shifted following dust deposition, with initial levels of <1.4% to a peak of 19.8% of the bacterial community (Westrich et al., 2016). A similar phenomenon was also observed in the surface waters of the mid-Atlantic with *Vibrio* populations increasing 1.5-fold in the mid-Atlantic following deposition (Westrich et al., 2018). In a follow up study in the Florida Keys, episodic dust events during a daily time series promoted a succession of bacterial responses, with declines in Prochlorococcus coinciding with initial increases in picoeukaryotes, followed by heterotrophic bacteria belonging to the order Vibrionales, and then subsequent shifts in response of different bacterial groups (Borchardt et al., 2020).

In each case, it has been hypothesized that dust-derived trace metals such as iron (Fe) plays a large role in supporting the growth of this otherwise conditionally rare bacterium. Fe is a trace metal that is essential for many enzymatic and metabolic processes including DNA precursors synthesis, photosynthesis, energy production, aerobic respiration, and nitrogen fixation (Payne et al., 2016; Westrich et al., 2016). Its essentiality for many microbial functions in combination with its tendency to transform into insoluble ferric hydroxide (rust), under alkaline and oxygenated conditions, makes the trace metal extremely limiting in marine environments (< 0.2nM at the ocean surface) (Payne et al., 2016). Bioavailable Fe can be transported to marine surface waters via riverine input, but the most significant source of Fe is from atmospheric deposition, which is estimated to be 3 times greater than that of riverine input, and supply up to 87% of dissolved iron to marine surface water communities (Conway & John, 2014; Duce & Tindale, 1991). Previous work has demonstrated significant increases in culturable *Vibrio*, including specific species *V. cholerae* and *V. alginolyticus*, following the addition of simulated dust and corresponding elevated Fe concentrations (Westrich et al., 2016).

Vibrio and a Changing Climate

Blooms of *Vibrio* and specific species that are known to be pathogenic towards humans can result in a higher risk of exposure to the public. In tandem with rising sea surface temperatures, *Vibrio* cases in humans have been increasing globally and expanding geographically (Baker-Austin et al., 2016; Froelich & Daines, 2020; McLaughlin et al., 2005; Newton et al., 2012). In 2004, a *V. parahaemolyticus* outbreak linked to raw oyster consumption occurred on a cruise ship in Alaska, extending by 1000km the northernmost documented outbreak due to *V. parahaemolyticus* in oysters.

Mean water temperatures at the oyster farm site had been increasing since 1997, and 2004 was the first year that the water temperatures did not drop below 15°C, allowing for substantial *Vibrio* growth and higher risk of exposure (McLaughlin et al., 2005). Additionally, following landfall of Hurricane Ian in Florida in September of 2022, a drastic increase in vibriosis cases occurred, 29 of which were associated with *V. vulnificus* (Sodders et al., 2023). Within the past year, there has been an increase in globally reported cholera outbreaks, with many reporting higher case numbers and fatalities (World Health Organization, 2016). Surveillance data indicates *Vibrio* related illnesses have more than doubled in the U.S since 1997 (CDC, 2023; Newton et al., 2012) (Figure 1.3).

Study Introduction

Outside of the well-studied role of temperature (and to some degree salinity), few environmental parameters exist that can be used to reliably predict favorable conditions for growth and exposure risk. Dust deposition may be able to serve as a predictor, but more work is needed to understand this. Microbial community dynamics in response to Saharan dust deposition have been described in certain oligotrophic settings (Borchardt et al., 2020; Westrich et al., 2016, 2018) but the role or effect of dust deposition is less clear regarding coastal waters where environmental parameters can be dynamic and the risk of human exposure is likely. The results from this study add a unique insight into the specific conditions that can elicit blooms of potentially harmful bacteria in nearshore coastal waters.

References:

Akhtar, R. (Ed.). (2020). *Extreme Weather Events and Human Health: International Case Studies*. Springer International Publishing. https://doi.org/10.1007/978-3-030-23773-8

Asplund, M. E., Rehnstam-Holm, A.-S., Atnur, V., Raghunath, P., Saravanan, V., Härnström, K., Collin, B., Karunasagar, I., & Godhe, A. (2011). Water column dynamics of Vibrio in relation to phytoplankton community composition and environmental conditions in a tropical coastal area. *Environmental Microbiology*, *13*(10), 2738–2751. https://doi.org/10.1111/j.1462-2920.2011.02545.x

Aunkham, A., Zahn, M., Kesireddy, A., Pothula, K. R., Schulte, A., Baslé, A., Kleinekathöfer, U., Suginta, W., & van den Berg, B. (2018). Structural basis for chitin acquisition by marine Vibrio species. *Nature Communications*, *9*(1), Article 1. https://doi.org/10.1038/s41467-017-02523-y

Baker-Austin, C., & Oliver, J. D. (2018). Vibrio vulnificus: New insights into a deadly opportunistic pathogen. *Environmental Microbiology*, *20*(2), 423–430. https://doi.org/10.1111/1462-2920.13955

Baker-Austin, C., Oliver, J. D., Alam, M., Ali, A., Waldor, M. K., Qadri, F., & Martinez-Urtaza, J. (2018). Vibrio spp. Infections. *Nature Reviews Disease Primers*, *4*(1), 1–19. https://doi.org/10.1038/s41572-018-0005-8

Baker-Austin, C., Trinanes, J. A., Salmenlinna, S., Löfdahl, M., Siitonen, A., Taylor, N. G. H., & Martinez-Urtaza, J. (2016). Heat Wave–Associated Vibriosis, Sweden and Finland, 2014. *Emerging Infectious Diseases*, *22*(7), 1216–1220. https://doi.org/10.3201/eid2207.151996

Baker-Austin, C., Trinanes, J., Gonzalez-Escalona, N., & Martinez-Urtaza, J. (2017). Non-Cholera Vibrios: The Microbial Barometer of Climate Change. *Trends in Microbiology*, *25*(1), 76–84. https://doi.org/10.1016/j.tim.2016.09.008

Ben-Haim, Y., & Rosenberg, E. (2002). A novel Vibrio sp. Pathogen of the coral Pocillopora damicornis. *Marine Biology*, *141*(1), 47–55. https://doi.org/10.1007/s00227-002-0797-6

Ben-Haim, Y., Zicherman-Keren, M., & Rosenberg, E. (2003). Temperature-Regulated Bleaching and Lysis of the Coral Pocillopora damicornis by the Novel Pathogen Vibrio coralliilyticus. *Applied and Environmental Microbiology*, *69*(7), 4236–4242. https://doi.org/10.1128/AEM.69.7.4236-4242.2003

Blackwell, K. D., & Oliver, J. D. (2008). The ecology of Vibrio vulnificus, Vibrio cholerae, and Vibrio parahaemolyticus in North Carolina Estuaries. *The Journal of Microbiology*, *46*(2), 146–153. https://doi.org/10.1007/s12275-007-0216-2

Böer, S. I., Heinemeyer, E.-A., Luden, K., Erler, R., Gerdts, G., Janssen, F., & Brennholt, N. (2013). Temporal and Spatial Distribution Patterns of Potentially Pathogenic Vibrio spp. At Recreational Beaches of the German North Sea. *Microbial Ecology*, *65*(4), 1052–1067. https://doi.org/10.1007/s00248-013-0221-4

Borchardt, T., Fisher, K. V., Ebling, A. M., Westrich, J. R., Xian, P., Holmes, C. D., Landing, W. M., Lipp, E. K., Wetz, M. S., & Ottesen, E. A. (2020). Saharan dust deposition initiates successional patterns among marine microbes in the Western Atlantic. *Limnology and Oceanography*, *65*(1), 191–203. https://doi.org/10.1002/lno.11291

Bristow, C. S., Hudson-Edwards, K. A., & Chappell, A. (2010). Fertilizing the Amazon and equatorial Atlantic with West African dust. *Geophysical Research Letters*, *37*(14). https://doi.org/10.1029/2010GL043486

Bross, M. H., Soch, K., Morales, R., & Mitchell, R. B. (2007). Vibrio vulnificus Infection: Diagnosis and Treatment. *American Family Physician*, *76*(4), 539–544.

CDC. (2019). *Vibrio species causing Vibriosis*. https://www.cdc.gov/vibrio/faq.html

CDC. (2023). *Pathogen Surveillance*. Centers for Disease Control and Prevention. https://www.cdc.gov/FoodNetFast

CDC Health Alert Network. (2023). *Severe Vibrio vulnificus Infections in the United States Associated with Warming Coastal Waters*. https://emergency.cdc.gov/han/2023/han00497.asp#:~:text=About%20150%E2%80%93200%20V.%20vulnificus,salt%20water%20and%20fresh%20water.

Coerdt, K. M., & Khachemoune, A. (2021). Vibrio vulnificus: Review of Mild to Life-threatening Skin Infections. *Cutis*, *107*(2). https://doi.org/10.12788/cutis.0183

Conway, T. M., & John, S. G. (2014). Quantification of dissolved iron sources to the North Atlantic Ocean. *Nature*, *511*(7508), Article 7508. https://doi.org/10.1038/nature13482

d'Almeida, G. A. (1986). A Model for Saharan Dust Transport. *Journal of Climate and Applied Meteorology*, *25*(7), 903–916. https://doi.org/10.1175/1520-0450(1986)025<0903:AMFSDT>2.0.CO;2

Daniels, N. A., MacKinnon, L., Bishop, R., Altekruse, S., Ray, B., Hammond, R. M., Thompson, S., Wilson, S., Bean, N. H., Griffin, P. M., & Slutsker, L. (2000).

Vibrio parahaemolyticus Infections in the United States, 1973–1998. *The Journal of Infectious Diseases*, *181*(5), 1661–1666. https://doi.org/10.1086/315459

Deshayes, S., Daurel, C., Cattoir, V., Parienti, J.-J., Quilici, M.-L., & de La Blanchardière, A. (2015). Non-O1, non-O139 Vibrio cholerae bacteraemia: Case report and literature review. *SpringerPlus*, *4*(1), 575. https://doi.org/10.1186/s40064-015-1346-3

Duce, R. A., & Tindale, N. W. (1991). Atmospheric transport of iron and its deposition in the ocean. *Limnology and Oceanography*, *36*(8), 1715–1726. https://doi.org/10.4319/lo.1991.36.8.1715

Eagon, R. G. (1962). *PSEUDOMONAS NATRIEGENS* , A MARINE BACTERIUM WITH A GENERATION TIME OF LESS THAN 10 MINUTES. *Journal of Bacteriology*, *83*(4), 736–737. https://doi.org/10.1128/jb.83.4.736-737.1962

Froelich, B. A., & Daines, D. A. (2020). In hot water: Effects of climate change on *Vibrio* –human interactions. *Environmental Microbiology*, *22*(10), 4101–4111. https://doi.org/10.1111/1462-2920.14967

Gilbert, J. A., Steele, J. A., Caporaso, J. G., Steinbrück, L., Reeder, J., Temperton, B., Huse, S., McHardy, A. C., Knight, R., Joint, I., Somerfield, P., Fuhrman, J. A., & Field, D. (2012). Defining seasonal marine microbial community dynamics. *The ISME Journal*, *6*(2), 298–308. https://doi.org/10.1038/ismej.2011.107

Goudie, A. S., & Middleton, N. J. (2001). Saharan dust storms: Nature and consequences. *Earth-Science Reviews*, *56*(1), 179–204. https://doi.org/10.1016/S0012-8252(01)00067-8

Greenfield, D. I., Gooch Moore, J., Stewart, J. R., Hilborn, E. D., George, B. J., Li, Q., Dickerson, J., Keppler, C. K., & Sandifer, P. A. (2017). Temporal and Environmental Factors Driving Vibrio Vulnificus and V. Parahaemolyticus Populations and Their Associations With Harmful Algal Blooms in South Carolina Detention Ponds and Receiving Tidal Creeks. *GeoHealth*, *1*(9), 306–317. https://doi.org/10.1002/2017GH000094

Griffin, D. W., Garrison, V. H., Herman, J. R., & Shinn, E. A. (2001). *African desert dust in the Caribbean atmosphere: Microbiology and public health*.

Hand, J. L., Mahowald, N. M., Chen, Y., Siefert, R. L., Luo, C., Subramaniam, A., & Fung, I. (2004). Estimates of atmospheric-processed soluble iron from observations and a global mineral aerosol model: Biogeochemical implications. *Journal of Geophysical Research: Atmospheres*, *109*(D17). https://doi.org/10.1029/2004JD004574

Heng, S.-P., Letchumanan, V., Deng, C.-Y., Ab Mutalib, N.-S., Khan, T. M., Chuah, L.-H., Chan, K.-G., Goh, B.-H., Pusparajah, P., & Lee, L.-H. (2017). Vibrio vulnificus: An Environmental and Clinical Burden. *Frontiers in Microbiology*, *8*, 997. https://doi.org/10.3389/fmicb.2017.00997

Horseman, M. A., & Surani, S. (2011). A comprehensive review of Vibrio vulnificus: An important cause of severe sepsis and skin and soft-tissue infection. *International Journal of Infectious Diseases*, *15*(3), e157–e166. https://doi.org/10.1016/j.ijid.2010.11.003

Hu, D., Liu, B., Feng, L., Ding, P., Guo, X., Wang, M., Cao, B., Reeves, P. R., & Wang, L. (2016). Origins of the current seventh cholera pandemic. *Proceedings of the*

National Academy of Sciences, *113*(48), E7730–E7739. https://doi.org/10.1073/pnas.1608732113

Ina-Salwany, M. Y., Al-saari, N., Mohamad, A., Mursidi, F.-A., Mohd-Aris, A., Amal, M. N. A., Kasai, H., Mino, S., Sawabe, T., & Zamri-Saad, M. (2019). Vibriosis in Fish: A Review on Disease Development and Prevention. *Journal of Aquatic Animal Health*, *31*(1), 3–22. https://doi.org/10.1002/aah.10045

Jensen, S., Frost, P., & Torsvik, V. L. (2009). The nonrandom microheterogeneity of 16S rRNA genes in *Vibrio splendidus* may reflect adaptation to versatile lifestyles. *FEMS Microbiology Letters*, *294*(2), 207–215. https://doi.org/10.1111/j.1574-6968.2009.01567.x

Kauffman, K. M., Hussain, F. A., Yang, J., Arevalo, P., Brown, J. M., Chang, W. K., VanInsberghe, D., Elsherbini, J., Sharma, R. S., Cutler, M. B., Kelly, L., & Polz, M. F. (2018). A major lineage of non-tailed dsDNA viruses as unrecognized killers of marine bacteria. *Nature*, *554*(7690), 118–122. https://doi.org/10.1038/nature25474

Kellogg, C. A., Griffin, D. W., Garrison, V. H., Peak, K. K., Royall, N., Smith, R. R., & Shinn, E. A. (2004). Characterization of Aerosolized Bacteria and Fungi From Desert Dust Events in Mali, West Africa. *Aerobiologia*, *20*(2), 99–110. https://doi.org/10.1023/B:AERO.0000032947.88335.bb

Koren, I., Kaufman, Y. J., Washington, R., Todd, M. C., Rudich, Y., Martins, J. V., & Rosenfeld, D. (2006). The Bodélé depression: A single spot in the Sahara that provides most of the mineral dust to the Amazon forest. *Environmental Research Letters*, *1*(1), 014005. https://doi.org/10.1088/1748-9326/1/1/014005

Maheshwari, M., Nelapati, K., & Kiranmayi, B. (2011). Vibrio cholerae—A Review. *Veterinary World*, 423. https://doi.org/10.5455/vetworld.2011.423-428

Mahowald, N. M., Baker, A. R., Bergametti, G., Brooks, N., Duce, R. A., Jickells, T. D., Kubilay, N., Prospero, J. M., & Tegen, I. (2005). Atmospheric global dust cycle and iron inputs to the ocean: ATMOSPHERIC IRON DEPOSITION. *Global Biogeochemical Cycles*, *19*(4). https://doi.org/10.1029/2004GB002402

Main, C. R., Salvitti, L. R., Whereat, E. B., & Coyne, K. J. (2015). Community-Level and Species-Specific Associations between Phytoplankton and Particle-Associated Vibrio Species in Delaware's Inland Bays. *Applied and Environmental Microbiology*, *81*(17), 5703–5713. https://doi.org/10.1128/AEM.00580-15

Munn, C. B. (2015). The Role of Vibrios in Diseases of Corals. *Microbiology Spectrum*, *3*(4), 10.1128/microbiolspec.ve-0006–2014. https://doi.org/10.1128/microbiolspec.ve-0006-2014

Newton, A., Kendall, M., Vugia, D. J., Henao, O. L., & Mahon, B. E. (2012). Increasing Rates of Vibriosis in the United States, 1996–2010: Review of Surveillance Data From 2 Systems. *Clinical Infectious Diseases : An Official Publication of the Infectious Diseases Society of America*, *54*(0 5), S391–S395. https://doi.org/10.1093/cid/cis243

Okada, K., Iida, T., Kita-Tsukamoto, K., & Honda, T. (2005). Vibrios Commonly Possess Two Chromosomes. *Journal of Bacteriology*, *187*(2), 752–757. https://doi.org/10.1128/JB.187.2.752-757.2005

Payne, S. M., Mey, A. R., & Wyckoff, E. E. (2015). Vibrio Iron Transport: Evolutionary Adaptation to Life in Multiple Environments. *Microbiology and Molecular Biology Reviews*, *80*(1), 69–90. https://doi.org/10.1128/mmbr.00046-15

Prospero, J. M. (1996). Saharan Dust Transport Over the North Atlantic Ocean and Mediterranean: An Overview. In S. Guerzoni & R. Chester (Eds.), *The Impact of Desert Dust Across the Mediterranean* (pp. 133–151). Springer Netherlands. https://doi.org/10.1007/978-94-017-3354-0_13

Prospero, J. M., Collard, F.-X., Molinié, J., & Jeannot, A. (2014). Characterizing the annual cycle of African dust transport to the Caribbean Basin and South America and its impact on the environment and air quality. *Global Biogeochemical Cycles*, *28*(7), 757–773. https://doi.org/10.1002/2013GB004802

Pruzzo, C., Vezzulli, L., & Colwell, R. R. (2008). Global impact of Vibrio cholerae interactions with chitin. *Environmental Microbiology*, *10*(6), 1400–1410. https://doi.org/10.1111/j.1462-2920.2007.01559.x

Ramírez-Camejo, L. A., Zuluaga-Montero, A., Morris, V., Rodríguez, J. A., Lázaro-Escudero, M. T., & Bayman, P. (2022). Fungal diversity in Sahara dust: Aspergillus sydowii and other opportunistic pathogens. *Aerobiologia*, *38*(3), 367–378. https://doi.org/10.1007/s10453-022-09752-9

Randa, M. A., Polz, M. F., & Lim, E. (2004). Effects of Temperature and Salinity on Vibrio vulnificus Population Dynamics as Assessed by Quantitative PCR. *Applied and Environmental Microbiology*, *70*(9), 5469–5476. https://doi.org/10.1128/AEM.70.9.5469-5476.2004

Richards, G. P., Watson, M. A., Needleman, D. S., Church, K. M., & Häse, C. C. (2015). Mortalities of Eastern and Pacific Oyster Larvae Caused by the Pathogens Vibrio coralliilyticus and Vibrio tubiashii. *Applied and Environmental Microbiology*, *81*(1), 292–297. https://doi.org/10.1128/AEM.02930-14

Ringgaard, S., Yang, W., Alvarado, A., Schirner, K., & Briegel, A. (2018). Chemotaxis Arrays in Vibrio Species and Their Intracellular Positioning by the ParC/ParP System. *Journal of Bacteriology*, *200*(15), 10.1128/jb.00793-17. https://doi.org/10.1128/jb.00793-17

Sampaio, A., Silva, V., Poeta, P., & Aonofriesei, F. (2022). Vibrio spp.: Life Strategies, Ecology, and Risks in a Changing Environment. *Diversity*, *14*(2), Article 2. https://doi.org/10.3390/d14020097

Schepanski, K., Tegen, I., & Macke, A. (2012). Comparison of satellite based observations of Saharan dust source areas. *Remote Sensing of Environment*, *123*, 90–97. https://doi.org/10.1016/j.rse.2012.03.019

Schryver, P. D., Defoirdt, T., & Sorgeloos, P. (2014). Early Mortality Syndrome Outbreaks: A Microbial Management Issue in Shrimp Farming? *PLOS Pathogens*, *10*(4), e1003919. https://doi.org/10.1371/journal.ppat.1003919

Shi, Z., Krom, M. D., Bonneville, S., Baker, A. R., Bristow, C., Drake, N., Mann, G., Carslaw, K., McQuaid, J. B., Jickells, T., & Benning, L. G. (2011). Influence of chemical weathering and aging of iron oxides on the potential iron solubility of Saharan dust during simulated atmospheric processing. *Global Biogeochemical Cycles*, *25*(2). https://doi.org/10.1029/2010GB003837

Slifka, K. M. J., Newton, A. E., & Mahon, B. E. (2017). Vibrio alginolyticus infections in the USA, 1988–2012. *Epidemiology & Infection*, *145*(7), 1491–1499. https://doi.org/10.1017/S0950268817000140

Sodders, N., Stockdale, K., Baker, K., Ghanem, A., Vieth, B., & Harder, T. (2023). Notes from the Field: Vibriosis Cases Associated with Flood Waters During and After Hurricane Ian — Florida, September–October 2022. *Morbidity and Mortality Weekly Report*, *72*(18), 497–498. https://doi.org/10.15585/mmwr.mm7218a5

Takemura, A., Chien, D., & Polz, M. (2014). Associations and dynamics of Vibrionaceae in the environment, from the genus to the population level. *Frontiers in Microbiology*, *5*. https://www.frontiersin.org/articles/10.3389/fmicb.2014.00038

Talbot, R. W., Harriss, R. C., Browell, E. V., Gregory, G. L., Sebacher, D. I., & Beck, S. M. (1986). Distribution and geochemistry of aerosols in the tropical north Atlantic troposphere: Relationship to Saharan dust. *Journal of Geophysical Research*, *91*(D4), 5173. https://doi.org/10.1029/JD091iD04p05173

Thompson, J. R., & Polz, M. F. (2006). Dynamics of *Vibrio* Populations and Their Role in Environmental Nutrient Cycling. In F. L. Thompson, B. Austin, & J. Swings (Eds.), *The Biology of Vibrios* (pp. 190–203). ASM Press. https://doi.org/10.1128/9781555815714.ch13

Thompson, J. R., Randa, M. A., Marcelino, L. A., Tomita-Mitchell, A., Lim, E., & Polz, M. F. (2004). Diversity and Dynamics of a North Atlantic Coastal Vibrio Community. *Applied and Environmental Microbiology*, *70*(7), 4103–4110. https://doi.org/10.1128/AEM.70.7.4103-4110.2004

Tran, L., Nunan, L., Redman, R., Mohney, L., Pantoja, C., Fitzsimmons, K., & Lightner, D. (2013). Determination of the infectious nature of the agent of acute hepatopancreatic necrosis syndrome affecting penaeid shrimp. *Diseases of Aquatic Organisms*, *105*(1), 45–55. https://doi.org/10.3354/dao02621

Turner, J. W., Good, B., Cole, D., & Lipp, E. K. (2009). Plankton composition and environmental factors contribute to Vibrio seasonality. *The ISME Journal*, *3*(9), Article 9. https://doi.org/10.1038/ismej.2009.50

Ushijima, B., Meyer, J. L., Thompson, S., Pitts, K., Marusich, M. F., Tittl, J., Weatherup, E., Reu, J., Wetzell, R., Aeby, G. S., Häse, C. C., & Paul, V. J. (2020). Disease Diagnostics and Potential Coinfections by Vibrio coralliilyticus During an Ongoing Coral Disease Outbreak in Florida. *Frontiers in Microbiology*, *11*. https://www.frontiersin.org/articles/10.3389/fmicb.2020.569354

van der Does, M., Korte, L. F., Munday, C. I., Brummer, G.-J. A., & Stuut, J.-B. W. (2016). Particle size traces modern Saharan dust transport and deposition across the equatorial North Atlantic. *Atmospheric Chemistry and Physics*, *16*(21), 13697–13710. https://doi.org/10.5194/acp-16-13697-2016

Westrich, J. R., Ebling, A. M., Landing, W. M., Joyner, J. L., Kemp, K. M., Griffin, D. W., & Lipp, E. K. (2016). Saharan dust nutrients promote *Vibrio* bloom formation in marine surface waters. *Proceedings of the National Academy of Sciences*, *113*(21), 5964–5969. https://doi.org/10.1073/pnas.1518080113

Westrich, J. R., Griffin, D. W., Westphal, D. L., & Lipp, E. K. (2018). Vibrio Population Dynamics in Mid-Atlantic Surface Waters during Saharan Dust Events. *Frontiers in Marine Science*, *5*, 12. https://doi.org/10.3389/fmars.2018.00012

World Health Organization. (2016). *Cholera – Global situation*. https://www.who.int/emergencies/disease-outbreak-news/item/2022-DON426

Zhang, X., Lin, H., Wang, X., & Austin, B. (2018). Significance of Vibrio species in the marine organic carbon cycle—A review. *Science China Earth Sciences*, *61*(10), 1357–1368. https://doi.org/10.1007/s11430-017-9229-x

Zhu, X. R., Prospero, J. M., & Millero, F. J. (1997). Diel variability of soluble Fe(II) and soluble total Fe in North African dust in the trade winds at Barbados. *Journal of Geophysical Research: Atmospheres*, *102*(D17), 21297–21305. https://doi.org/10.1029/97JD01313

Figures:

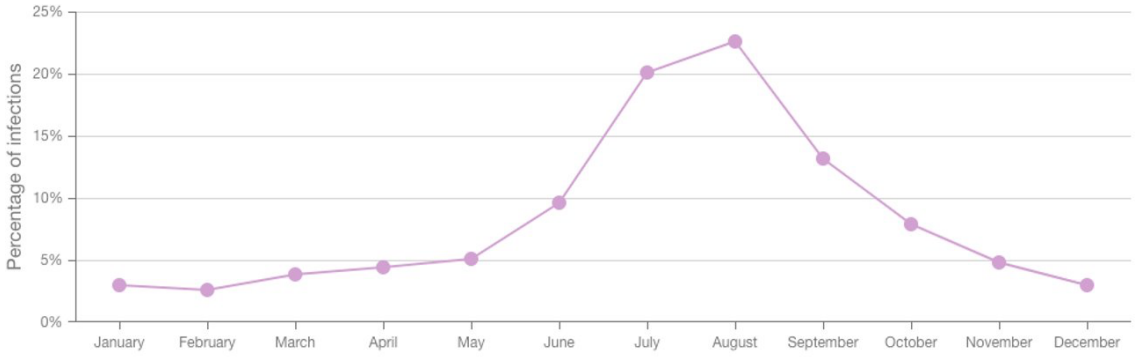

Figure 1.1: *Vibrio* infections by month displaying notably higher percentage of infections between May and October (CDC, 2023).

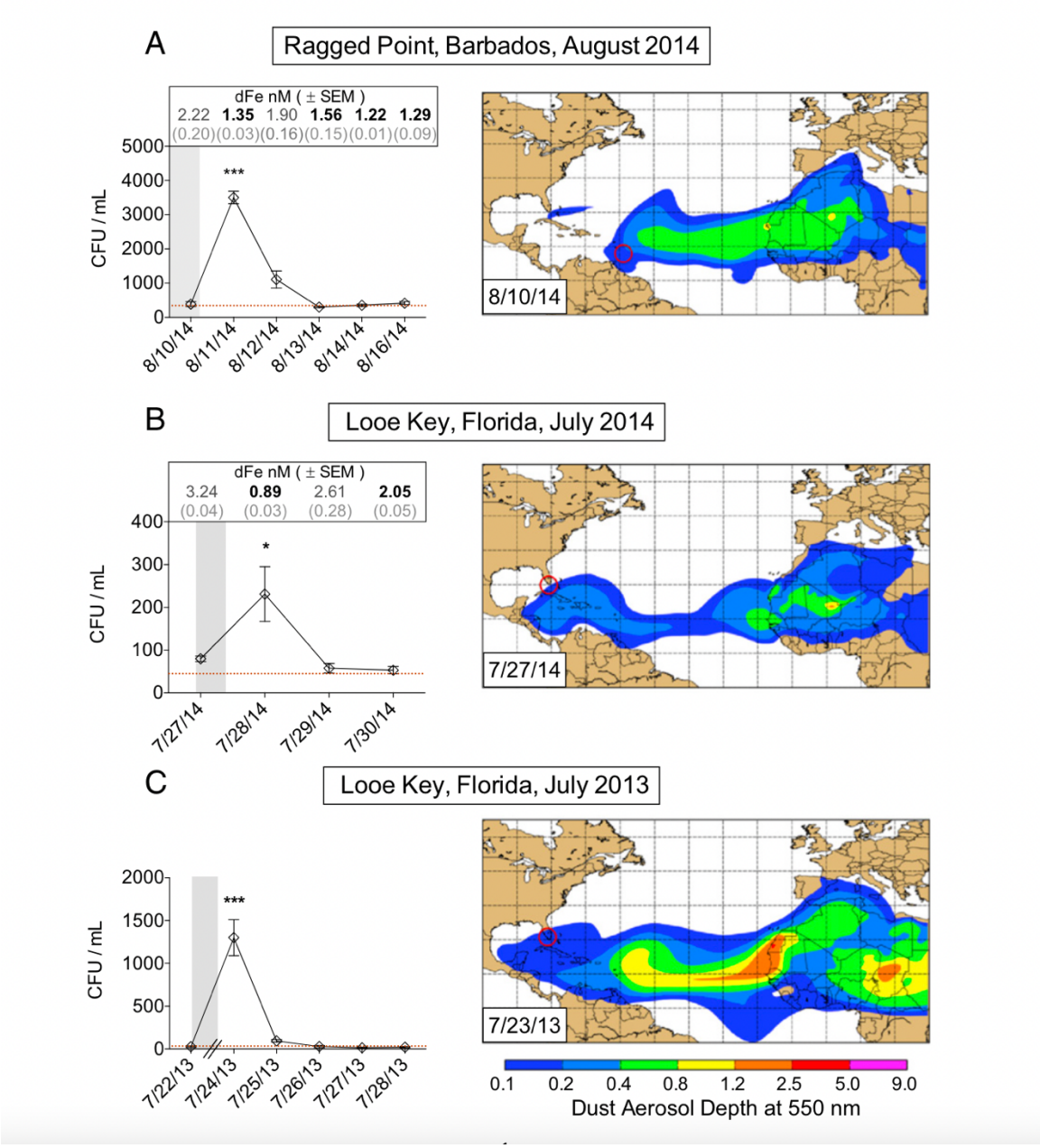

Figure 1.2: *Vibrio* concentrations (CFU mL^{-1}) in response to Saharan dust deposition (grey bar) in the Barbados and Florida Keys (Westrich et al., 2016).

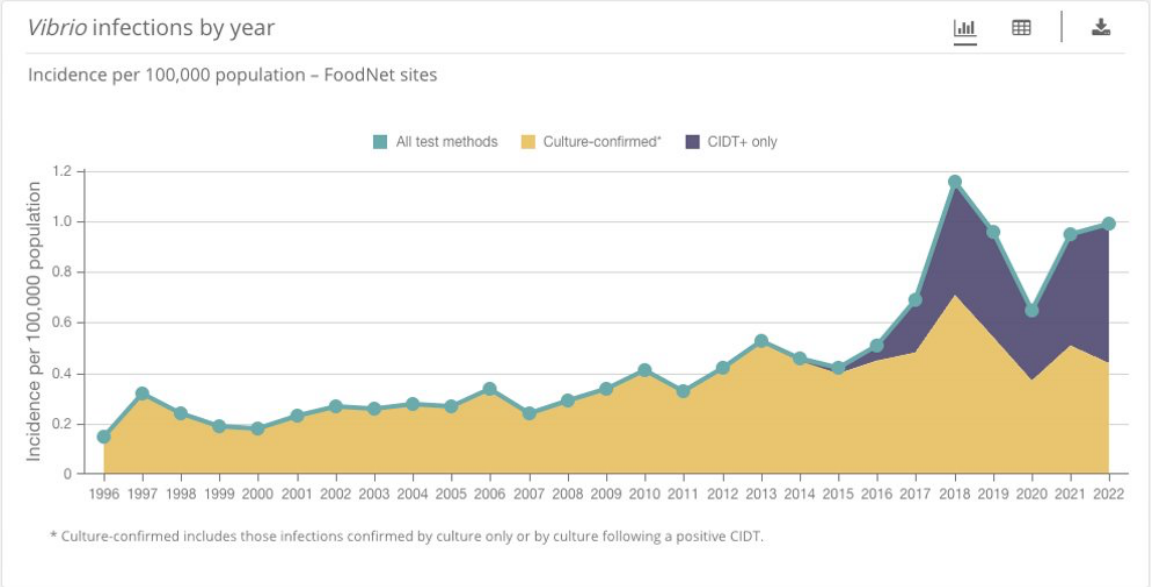

Figure 1.3: *Vibrio* infections by year (incidence per 100,000 population).Yellow shading indicates culture-confirmed cases, purple shading indicates culture-independent confirmation, and the blue line indicates all test methods (CDC, 2023).

CHAPTER 2

THE INTERACTING EFFECTS OF LOCAL CONDITIONS AND SAHARAN DUST DEPOSITION ON *VIBRIO* POPULATION DYNAMICS IN NEARSHORE COASTAL WATERS [1]

[1] Greenslit, N.W., Manalilkada Sasidharan, S., Urutia, F., Wetz, M.S., & Lipp, E.K. To be submitted to *Applied and Environmental Microbiology*.

Abstract:

Each summer, episodic plumes of Saharan dust travel across the Atlantic to be deposited in the surface waters of the Gulf of Mexico. Dust aerosols have been shown to serve as a significant source of nutrients that can potentially facilitate the development of microbial blooms (including *Vibrio*) in offshore and pelagic environments. However, the potential effect of deposition events in more dynamic inland coastal waters is not known. This study aimed to quantify *Vibrio* population dynamics and composition in response to dust events in regions where environmental parameters are more variable, and human risk of exposure is higher. Samples were collected daily from three distinct sites near Corpus Christi, TX (USA) for 12 days during the summer of 2022, capturing periods before, during, and after a Saharan dust event. During dust days, total *Vibrio* concentrations (copies mL^{-1}) increased significantly at two of the three sites ($p < 0.05$), with greatest increase noted at the Gulf of Mexico beach site (2.7×10^3 to 2.3×10^4 copies mL^{-1}). Among the individual species, *V. vulnificus* and *V. cholerae* were correlated with dust levels (aerosol optical density) ($p \leq 0.007$) at Blind Oso Bay, but this was likely due to the combinatory effects of dust influx and potential wastewater discharge. This study provides an increased understanding of the conditions that can elicit blooms of *Vibrio* in coastal and inland regions where risk of human exposure is more likely.

Introduction:

The Sahara Desert is a significant source of atmospheric dust, eliciting an estimated 800 Tg yr^{-1} each year (Goudie & Middleton, 2001). Plumes of this dust travel across the Mediterranean, reaching Europe and parts of the Middle East, with a majority travelling west across the Atlantic via the trade winds to be deposited in the surface waters of the Atlantic, Caribbean, and Gulf of Mexico. These dust events are highly episodic, occurring 3- 4 times a year typically in the summer months and lasting 3-5 days each. Dust aerosols can harbor a wide diversity of bacteria (Kellogg et al., 2004), fungi (Ramírez-Camejo et al., 2022), virus-like particles (Griffin et al., 2001), and minerals (Formenti, 2003), and also serve as a significant source of macro and micronutrients such as phosphate (PO_4^{3-}), ammonium (NH_4^+), nitrate (NO_3^-), and iron (Fe) (Goudie & Middleton, 2001; Graham & Duce, 1982; Mills et al., 2004; Savoie et al., 1989). This addition of otherwise limiting resources has been found to lead to blooms of certain microbial groups, including nitrogen-fixing *Trichodesmium* cyanobacteria and subsequent blooms of harmful algal species *Karenia brevis* in the Gulf of Mexico (Lenes et al., 2008), increases in abundance of *Synechococcus* in the Mediterranean Sea (Herut et al., 2005), and increases of heterotrophic bacteria (including Flavobacteriacea, *Gammaproteobacteria* and *Bacteroidetes*) in the Atlantic and Mediterranean (Laghdass et al., 2011; Lekunberri et al., 2010; Marañon et al., 2010; Reche et al., 2009). Of the heterotrophic responders, emerging evidence has shown increases in *Vibrio* abundance following the episodic influx of limiting resources and substrate, resulting in blooms of bacteria that are associated with disease (Borchardt et al., 2020; Westrich et al., 2016, 2018).

Bacteria belonging to the genus *Vibrio* are opportunistic heterotrophs that are ubiquitous in marine, estuarine, and freshwater environments. *Vibrio* include a range of species pathogenic to humans and marine organisms (Baker-Austin et al., 2018; Ben-Haim, Thompson, et al., 2003; Ina-Salwany et al., 2019; Richards et al., 2015; Tran et al., 2013; Ushijima et al., 2020b). In humans, any infection due to species of the *Vibrionaceae* family is notifiable in the U.S. (CDC, 2019), with *V. alginolyticus*, *V. cholerae*, *V. parahaemolyticus*, and *V. vulnificus* being the most common cause of illness (CDC, 2023). Infections primarily occur through either an oral route via the consumption of raw or uncooked seafood such as oysters (or contaminated drinking water in the case of *V. cholerae*) or through direct exposure (e.g., swimming or wading).

Traditionally, case prevalence tends to be highest in the summer months, as *Vibrio* infections are associated with warmer waters (CDC, 2019). Over the past few decades however, a geographical and seasonal expansion has been observed in tandem with rising sea surface temperatures (Baker-Austin et al., 2016; Froelich & Daines, 2020; McLaughlin et al., 2005), with surveillance data indicating *Vibrio* related illnesses have more than doubled in the U.S. since 1997 (CDC, 2023; Newton et al., 2012). Though ubiquitous constituents of marine and brackish environments, *Vibrio* are considered conditionally rare, as they comprise <1% of the microbial community (Shade et al., 2014; Thompson et al., 2004). Under the proper conditions however, the bacteria can rapidly bloom to make up a large percentage of the community over a short period of time (Westrich et al., 2016, 2018), greatly enhancing risk of exposure. This calls for a need to better understand what specific factors may drive these blooms, and when elevated exposure risk is likely.

Of the environmental correlates that are associated broadly with *Vibrio* abundance, temperature and salinity are the most prominent, with optimal ranges for growth at temperatures >18°C and moderately saline waters (Froelich & Daines, 2020). When it comes to specific species, physiochemical tolerances can vary, with some species preferring salinities ≤ 10 (e.g., *V. cholerae* and *V. vulnificus*), and others having a more broad environmental tolerance (e.g., *V. parahaemolyticus* and *V. alginolyticus*) (Norfolk, 2023; Randa et al., 2004; Takemura et al., 2014). Biotic factors like plankton abundance are also known to be important correlates of *Vibrio* abundance as they are capable of utilizing the chitinous exoskeletons of zooplankton and organic nutrients derived from passive leaking or senescence of phytoplankton (Greenfield et al., 2017; Pruzzo et al., 2008; Turner et al., 2009). Increases in *Vibrio* abundance and case incidence have previously been documented following environmental fluctuations such as increases in DOM from harmful algal blooms (Greenfield et al., 2017), heat waves (Baker-Austin et al., 2016), and hurricanes (Sodders et al., 2023), with recent evidence pointing towards *Vibrio* blooms in response to Saharan dust deposition events (Borchardt et al., 2020; Westrich et al., 2016, 2018).

Previous work has characterized *Vibrio* blooms in response to Saharan dust input in the oligotrophic settings of the Caribbean (Florida Keys), subtropical Atlantic (Barbados), and mid-Atlantic (North Pond) with surface water concentrations of total *Vibrio* increasing by five to thirty times that found during non-dust conditions and returning to baseline levels within 24-48 hours (Westrich et al., 2016, 2018). *Vibrio* composition within the larger microbial community also shifted following dust deposition, with initial levels of <1.4% to a peak of 19.8% of the bacterial community

(Westrich et al., 2016). A similar phenomenon was also observed in the surface waters of the tropical and open ocean mid-Atlantic with *Vibrio* populations increasing 1.5-fold in the mid-Atlantic following deposition (Westrich et al., 2018). In a follow up study in the Florida Keys, episodic dust events during a daily time series promoted a succession of bacterial responses, with declines in *Prochlorococcus* coinciding with initial increases in bacteria belonging to the order *Vibrionales*, followed by subsequent shifts in response of different bacterial groups (Borchardt et al., 2020).

To date, our understanding of *Vibrio* and other microbial response to dust input has focused on oligotrophic offshore or pelagic settings, where dust input is considered to be a critical source of limiting nutrients, and Fe in particular. It is unknown how comparable these findings are to nearshore coastal areas where environmental parameters (e.g., nutrients, salinities) are more dynamic (and in terms of human health relevance, the risk of exposure is considerably higher). The composition of desert dust aerosols can be complex and may have the potential to deliver critical resources that could be more readily exploited by opportunistic bacteria (like *Vibrio*) and elicit a population bloom despite a more dynamic environmental setting. During these bloom periods, human exposure through recreation or the consumption of raw seafood may be more likely, presenting a risk to the public health. To better understand *Vibrio* dynamics following dust deposition in nearshore coastal regions, a high frequency time series capturing a dust event was conducted in July 2022 in Corpus Christi, Texas (USA). This study aimed to quantify *Vibrio* population dynamics and composition in response to dust input in inland and nearshore coastal waters where baseline dynamics may be more variable, and risk of human exposure is high.

Materials and Methods:

Site Description

Sampling took place at three locations in Corpus Christi, TX: Blind Oso Bay, a residential canal system on Padre Island, and a beach site on the Gulf of Mexico (Figure 2.1). Sites were chosen to represent inland coastal (Blind Oso and Canals) and nearshore coastal (Gulf) regions. Blind Oso Bay is a shallow tributary (depth: 0.4-1m) that is popular amongst wade-fishermen and kayakers. Throughout the year, the Bay experiences fluctuating salinities (~24-37) and high levels of nutrients and chlorophyll-*a* due in part to wastewater treatment discharge (Wetz, 2014; Wetz et al., 2016; Manalilkada Sasidharan et al., In Progress) (Table S1). Additionally, the Bay has persistent issues with high levels of fecal indicator bacteria, placing it on the U.S. impaired waters list (Nicolau & Hill, 2013; Texas Commission on Environmental Quality, 2022). The Canals site (depth: 1.2-1.7m) experiences salinities that are primarily driven by precipitation with ranges from ~29-46 (Manalilkada Sasidharan et al., In Progress) (Table S1), and highest values in the summer months. Kayakers and occasional swimmers can be found at this location. The Gulf site (depth: 0.1-1.5m) is popular with fisherman and beach goers and is characterized by salinities ranging from ~29-37 with near constant levels (~35-37) during the summer, and relatively low baseline nutrient levels (Manalilkada Sasidharan et al., In Progress) (Table S1).

Sample Collection and Processing

Samples were collected daily between 7:00 and 10:30 a.m. local time from July 7th through July 19th, 2022 at each site, with the exception of July 10, when no sample was obtained. Samples were collected from just below the surface in duplicate in sterile

1L and 250 mL polypropylene bottles for molecular and culturable *Vibrio* analyses, respectively. For nutrient and chlorophyll-*a* analysis, samples were collected in acid-washed amber wide-mouth plastic bottles and kept on ice until processing. Samples for culturable *Vibrio* analysis were stored in a cooler containing ambient seawater to avoid cooling that could result in non-culturable cells. Samples for molecular analysis were stored on ice. All samples were transported and analyzed in the lab within 2 h of collection.

Water Quality Analysis

Up to 45 mL of the samples were filtered through clean, pre-combusted (450°C for 24 h) 25mm (0.7μm) glass fiber filters (grade GF/F), and filtrate was collected in clean acid-washed bottles for the analysis of dissolved nutrients. All samples were preserved in duplicate and stored frozen (-20°C) until analysis. Following Standard Methods (*APHA: Standard Methods for the Examination of Water and Wastewater.*, 2005) ammonium (NH_4^+), nitrate + nitrite ($NO_3^- + NO_2^-$), orthophosphate (PO_4^{3-}), and silicate (SiO_4^{2-}) were determined using a Seal QuAAtr® auto-analyzer. 15 mL of unfiltered samples were used for measuring TOC and TN. Dissolved organic carbon (DOC), total organic carbon (TOC), total nitrogen (TN), and total dissolved nitrogen (TDN) were measured using a Shimadzu® TOC-V TN-1 module (ASTM 2015) with self-contained magnetic stirrers. 25 mL of sample was filtered (<5 mm Hg) through clean 25 mm Whatman® GF/F filters and stored in 3 mL vacutainers (BD Vacutainer®: Cat#366668) for chlorophyll-*a* analysis which was measured using a fluorometer (Wetz et al. 2016). Dissolved inorganic nitrogen (DIN) was estimated as the sum of NH_4^+ and $NO_3^- + NO_2^-$ concentrations. Dissolved organic nitrogen (DON) was

estimated as the difference between TDN and DIN. PO_4^{3-} concentration was estimated as dissolved inorganic phosphorus (DIP). The proportion of DIN to DIP (DIN: DIP) was then calculated. The details of the analytical procedures, including standard protocols, instrument calibration, standards used, blanks, and quality control, can be referred from the previously published literature from the Wetz laboratory (Hayes, 2020; Walker et al., 2020; Wetz et al., 2016, 2017). For the analysis of total suspended sediment (TSS), 200 mL of unfiltered sample were concentrated on pre-rinsed and pre-combusted (450°C) 47mm 0.7µm pore size glass fiber filters (GF/F) and dried at 60°C for 12-15 hours. Weight difference was calculated as the difference between the GF/F containing dried sample and clean GF/F (recorded prior to adding sample). Finally, TSS (mg L^{-1}) was calculated as the weight difference divided by the total volume of filtered sample (mL) multiplied by 10^6.

Culturable Vibrio

To serve as an initial metric of *Vibrio* dynamics during the time series, *Vibrio* bacteria were enumerated via spread plating 100µL of sample water in triplicate onto selective thiosulfate-citrate-bile salts-sucrose (TCBS) Cholera Medium agar (Cat#: OXCM0333B; Thermo Scientific). Additionally, 100µL of a 1:10 dilution (in sterile phosphate buffered saline) was plated in triplicate for each sample. Following incubation at 30°C for 18-24 hours, all yellow and green colonies were counted as *Vibrio*, enumerated as colony forming units (CFU) mL^{-1}, and compared across sites and dates.

DNA Extraction and quantitative PCR (qPCR)

Upon arrival in the lab, up to 100 mL of sampled water was concentrated onto 0.2 µm pore size 47 mm diameter polycarbonate membranes (Isopore, Millipore) via vacuum

filtration and stored at -80°C until ready for use. Total DNA was extracted directly from membranes using a ZymoBIOMICS DNA Miniprep Kit (Cat#: D4300; ZYMO RESEARCH), according to the manufacturer's instructions. All extracts were eluted in 100 µl PCR-grade water (Cat#: 46-000-CM; Thomas Scientific). Final extracts were stored at -20°C for molecular analysis. qPCR was used to estimate abundances of total *Vibrio* as well as specific species (*V. alginolyticus*, *V. cholerae*, *V. vulnificus*, and *V. parahaemolyticus*), and total bacteria (Table S2-S4). Due to its proximity to the Oso Wastewater Treatment Plant (WWTP), the human fecal marker (HF183) was also analyzed by qPCR in all Blind Oso samples to assess potential wastewater discharge (Table S2-S4).

Reaction mixtures and cycling conditions were conducted according to the references in Table S3-S4 with slight modifications. Each run using SYBR PowerUp PCR Mastermix (Cat#: A25742; Applied Biosystems) was followed by a dissociation step (60°C to 95°C at 0.5°C/cycle intervals) to determine a melt curve for amplification specificity. A positive (G-block diluted to approximately 10^3 gene copies μL^{-1}) and non-template control (molecular-grade water) were included on each run. All qPCR reactions were run in triplicate (technical replicates) on a CFX96 Touch Real-Time PCR Detection System (Bio-Rad), with the exception of *V. cholerae* at Blind Oso, which displayed large variation between triplicates, and thus had 5 technical replicates. Reaction inhibition tests were conducted by inoculating approximately 10^3 target gene copies μL^{-1} of the corresponding G-block into 10% of the samples. In the case of inhibition, samples were diluted up to 1:50 and re-run. For assays targeting *V. parahaemolyticus* and *V. vulnificus*, an internal amplification control (IAC) was diluted to achieve Cq values between 23-26

to assess amplification efficiency (Jones, 2022). All qPCR data were reported as copies μL^{-1} and cycle threshold (*Cq*) values were compared to linearized standard curves with the final qPCR data reported as copies mL^{-1} after considering the volume of original sample that was extracted. Limit of detection (LOD) for each assay was determined by running linearized standard (G-block) in 5 technical replicates serially diluted from 10^6 to 10^{-1} gene copies μL^{-1}. The number of technical replicates that amplified at each serial dilution was determined and a probit model was used to compute the effective dose of template that was required to achieve a given probability (95%) of observing a positive qPCR assay (Merkes et al., 2019) (Figure S1). Any probit assay that yielded a LOD < 1 copy μL^{-1} was assigned the theoretical LOD of 3 copies μL^{-1} (Bustin et al., 2009). Any qPCR replicate below the LOD for any target, was assigned a value of 50% the LOD.

Dust Aerosols

Aerosol optical depth (AOD) for all types of aerosols were determined in 6 h intervals for the duration of the time series for a 1°x1° (latitude and longitude) grid including the three sites in Corpus Christi via the Navy Aerosol Analysis and Prediction System (NAAPS) Reanalysis (Lynch et al., 2016), Naval Research Laboratory. The dust specific AOD was extracted, and a composite sum was calculated for the 24 h period preceding the time of sample collection. The resolution of data required that the same AOD values were used for all three sites, as all three sampling sites were within one 1° latitude by 1° longitude model grid. Dust aerosol source was confirmed through the NAAPS-RA day-to-day dust AOD distribution maps, and NOAA's HYSPLIT Trajectory Model (Stein et al., 2015) (Figure S2).

Statistics

All statistical analyses were conducted in R and R Studio (R Core Team, 2022; R Studio Team, 2022). Data were visualized using ggplot2 (Wickham, 2016). Shapiro-Wilk's normality tests were conducted in R to determine distributions of variables. For culture counts, the dilution (i.e., undiluted or 1:10 dilution) that displayed the least variance between CFU counts among sample triplicates were selected and the mean was reported as CFU mL^{-1}.

Correlations using Spearman's ρ between all abiotic and biotic variables were calculated using the Hmisc package (Harrell, 2023) and plotted as heatmaps with the corrplot package (Wei & Simko, 2021). Due to variability in distribution among the variables, all data was analyzed raw with no transformations. For correlation analysis, all biological and technical replicates were averaged, and tests were run on each site individually. For all analyses, a p-value ≤ 0.05 was considered significant. The timeseries was split into low dust days (AOD ≤ 0.13) (July 7^{th} – July 12^{th}) and high dust days (AOD ≥ 0.17) (July 13^{th} – July 19^{th}) and means in total *Vibrio,* each *Vibrio* species, culturable *Vibrio,* and total bacteria were compared across sites and by dust condition. T-tests were used on variables that were normally distributed (total *Vibrio*, culturable *Vibrio*), and Wilcoxon tests were used on variables that were non-parametric (total bacteria, *Vibrio* species). Using the means between low and high dust days, fold-changes were calculated by subtracting the low dust average from the high dust average and dividing by the low dust average. To identify any initial lagged relationship between dust deposition and *Vibrio* levels, a cross-correlation analysis was run between dust AOD and enumerated *Vibrio* (CFU mL^{-1} and copies mL^{-1} for both total *Vibrio* and species) by site using the ccf function in R. To visualize site specific dynamics in environmental correlates of *Vibrio*

(CFU mL^{-1} and copies mL^{-1}), a principal component analysis (PCA) was conducted and visualized in R using the FactoMineR (Lê et al., 2008) and factoextra (Kassambara & Mundt, 2020) packages respectively. Data was grouped by site, point size was assigned to dust AOD, and included variables that were chosen based on (1) significant relationships from Spearman's correlation analysis, and (2) well established environmental correlates of total *Vibrio*.

Results:

Dust aerosols

At the beginning of the time series (July 7th-July 12th), dust AOD (calculated as a 24-hour composite sum) had an average value of 0.095. An initial peak in dust AOD was observed on July 13th (AOD = 0.2), followed by a drastic increase on July 16th reaching an AOD of 0.57. Dust AOD remained elevated (AOD = 0.55) until July 19th, when levels were observed to decrease (AOD = 0.17) (Figure 2.2).

Water quality

Abiotic and biotic environmental variables varied by site. No precipitation occurred during the time series. Average water temperatures were 31°C at the Canals, 28°C at the Gulf, 29°C at Blind Oso. Throughout the timeseries salinity was comparably higher (~40 – 43) at the Canals, moderate at the Gulf (35-37), and notably variable at Blind Oso decreasing from ~41 (July 11th) to ~20 (July 19th), coinciding with dust deposition (Figure 2.3). DO (mg L^{-1}) levels were lowest at the Canals (average: 3.01 mg L^{-1}) followed by the Gulf (average: 5.98 mg L^{-1}), and Blind Oso (average: 7.3 mg L^{-1}). At Blind Oso, DO levels displayed elevated levels from July 15th to July 19th, reaching a peak of 9.44 mg L^{-1} on July 16th (Figure 2.3). PO_4^{3-} concentrations were relatively low at

the Canals and Gulf (averages: <0.5 μM), with the exception of a local spike occurring on July 16th (1.56 μM) at the Canals. At Blind Oso, PO_4^{3-} concentrations (average: 3.1 μM), exhibited elevated levels beginning on July 17th and remained elevated for the remainder of the timeseries, reaching a peak on July 19th (9.24 μM) (Figure 2.3). Nitrogen species were highest at Blind Oso, exhibiting elevated levels during the latter half of the time series, barring NH_4^+ where a consistent trend (temporally and in magnitude) was observed across all sites with local peaks occurring on July 14th at the Canals (2.75 μM), July 15th at the Gulf (2.24 μM), and July 16th at Blind Oso (1.73 μM) respectively (Figure 2.3). TOC was highest at Blind Oso (average: 1431 μM) as compared to the Gulf (average: 260 μM) and Canals (average: 760 μM). TOC concentrations increased at Blind Oso beginning on July 12th reaching a value of 2077 μM on July 18th. TSS levels averaged at 51.3 mg L^{-1} and 79.9 mg L^{-1} at the Canals and Gulf respectively, while Blind Oso was comparably higher (average: 243.4 mg L^{-1}) with notable peaks occurred on July 12th (346.4 mg L^{-1}) and July 17th (400 mg L^{-1}) (Figure 2.3).

Chlorophyll-*a* averaged at 4.43 μg L^{-1} and 7.89 μg L^{-1} at the Gulf and Canals respectively, with levels slightly increasing throughout the time series. Chlorophyll-*a* was comparably higher at Blind Oso (average: 41.87 μg L^{-1}), with concentrations increasing beginning on July 12th and continuing for the rest of the time series (Figure 2.3). At Blind Oso, chlorophyll-*a* was strongly correlated with nutrients DIN ($\rho = 0.69$, $p = 0.01$), TDN ($\rho = 0.58$, $p = 0.05$), and TOC ($\rho = 0.71$, $p = 0.009$) (Figure 2.4) while at the Canals, there was a close association with NH_4^+ ($\rho = 0.59$, $p = 0.04$) and TSS ($\rho = 0.60$, $p = 0.04$) (Figure 2.5). At the Gulf, chlorophyll-*a* had significant correlations with nutrients NH_4^+ ($\rho = 0.71$, $p = 0.01$) and DIN ($\rho = 0.73$, $p = 0.007$) (Figure 2.6). Human fecal

contamination analysis at Blind Oso revealed an increase in HF183 gene copies mL^{-1} beginning on July 13th, from initial levels below the limit of detection to a peak on July 18th (7.5×10^6 gene copies mL^{-1}) (Figure S3). HF183 concentrations were negatively correlated with salinity ($\rho = -0.70$, $p = 0.01$) and positively correlated with DO ($\rho = 0.68$, $p = 0.02$) and nutrients including TDN ($\rho = 0.83$, $p < 0.001$), TN ($\rho = 0.75$, $p = 0.005$), TOC ($\rho = 0.76$, $p = 0.004$), as well as total bacteria ($\rho = 0.62$, $p = 0.03$) (Figure 2.4).

Microbial analysis

Across all sites, culturable *Vibrio* (CFU mL^{-1}) were low and/or variable through July 14th. During what were classified as high dust influx days (July 13th- July 19th), *Vibrio* CFU mL^{-1} were observed to increase at all sites with the greatest increase at the Gulf, reaching a peak of 1,550 CFU mL^{-1} on July 15th. Local peaks in CFU mL^{-1} occurred on July 16th at Blind Oso (777 CFU mL^{-1}) and the Canals (817 CFU mL^{-1}) (Figure 2.2). When lagged by 24 h (dust aerosols preceding change in *Vibrio* concentration by 24 h) (Figure S4), culturable *Vibrio* were significantly correlated with dust AOD at the Gulf ($\rho = 0.71$, $p = 0.01$) (Figure 2.6). *Vibrio* CFU mL^{-1} continued to remain elevated for the rest of the time series at the Gulf but declined at the two other sites as dust influx decreased (Figure 2.2).

Cross-correlation analysis revealed that total *Vibrio* levels (copies mL^{-1}) had the strongest initial responses to dust aerosols when lagged by 24 h (Figure S5) for both the Gulf ($\rho = 0.65$, $p = 0.02$) and Blind Oso ($\rho = 0.70$, $p = 0.01$) (Figures 2.4, 2.6) increasing 7.7-fold ($p < 0.001$) and 0.74-fold ($p = 0.04$) during high dust days respectively (Figure 2.2)**.** Beginning on July 12th, total *Vibrio* at the Gulf began increasing reaching an initial peak of 2.8×10^4 copies mL^{-1} on July 15th, while a second higher peak was observed on

July 18th (3.7 x 10^4 copies mL^{-1}) (Figure 2.2). In addition to a 24 h lag to dust, total *Vibrio* levels at the Gulf site were strongly correlated with day-of dust AOD ($\rho = 0.67$, $p = 0.02$), chlorophyll-*a* ($\rho = 0.84$, $p < 0.001$), total bacteria ($\rho = 0.67$, $p = 0.02$), NH_4^+ ($\rho = 0.90$, $p < 0.001$), and DIN ($\rho = 0.91$, $p < 0.001$) (Figure 2.6). At Blind Oso, total *Vibrio* increased to a local peak of 2.1 x 10^4 copies mL^{-1} on July 14th and remained elevated for the remainder of the time series (Figure 2.2). Total *Vibrio* at Blind Oso did not correlate with any other variables aside from a 24 h lag to dust AOD. Throughout the time series, the Canals exhibited a small, but insignificant increase in total *Vibrio* with no noticeable response to dust aerosols (Figure 2.2).

Specific *Vibrio* species varied considerably between species and by site. Across all sites and dates *V. vulnificus* was most commonly detected (63.9% positive; 23/36 samples), followed by *V. cholerae* (31% positive; 11/36 samples). *V alginolyticus* and *V. parahaemolyticus* were least commonly detected at only 11% of samples positive (4/36, each). Gene copies mL^{-1} of *V. alginolyticus* and *V. parahaemolyticus* were either below the detection limit or in very low abundance. Concentrations of *V. cholerae* and *V. vulnificus* were relatively low at the beginning of the timeseries across sites. During heavy dust days (July 13th-July 19th), *V. cholerae* exhibited a significant 3.2-fold increase at Blind Oso ($p = 0.03$) and *V. vulnificus* significantly increased 6.5-fold at Blind Oso ($p = 0.02$), reaching up to 7555 and 206 copies mL^{-1} respectively (Figure 2.7). *V. cholerae* concentrations at Blind Oso were highly variable between technical replicates. Throughout the time series, abundances of *V. vulnificus* remained low and variable at the Canals and the Gulf. Two peaks in *V. cholerae* occurred at the Canals on July 12th (preceding light dust influx on July 13th) and July 15th (Figure 2.7) and two peaks were

observed at the Gulf on July 17th and July 19th (following heavy dust influx). Cross-correlation analysis showed variability among species and sites (Figure S6). At Blind Oso, *V. cholerae* had significant correlations with a 0 h lag to dust ($\rho = 0.75$, $p = 0.005$) and a 24 h lag to dust ($\rho = 0.73$, $p = 0.007$). Additionally, *V. cholerae* at Blind Oso had significant correlations with TN ($\rho = 0.85$, $p < 0.001$), TOC ($\rho = 0.77$, $p = 0.003$), DO ($\rho = 0.66$, $p = 0.02$), and a negative correlation with salinity ($\rho = -0.69$, $p = 0.01$). *V. vulnificus* at Blind Oso exhibited significant relationships with both 0 h ($\rho = 0.73$, $p = 0.007$), and 24 h lag to dust AOD ($\rho = 0.84$, $p < 0.001$) (Figures 2.4). *V. vulnificus* at Blind Oso exhibited a strong negative association with salinity ($\rho = -0.85$, $p < 0.001$), a positive correlation with DO ($\rho = 0.76$, $p = 0.004$), and strong correlations with nutrients including NH_4^+ ($\rho = 0.67$, $p = 0.02$), DIN ($\rho = 0.71$, $p = 0.01$), TDN ($\rho = 0.79$, $p = 0.002$), TOC ($\rho = 0.64$, $p = 0.02$), and TN ($\rho = 0.71$, $p = 0.009$). *V. vulnificus* also significantly correlated with HF183 ($\rho = 0.68$, $p = 0.02$) and total bacteria ($\rho = 0.60$, $p = 0.04$) (Figure 2.4).

On average, total bacteria was highest at Blind Oso (2×10^7 copies mL^{-1}) while concentrations were lower by order(s) of magnitude at the Gulf (8.2×10^5 copies mL^{-1}) and Canals (1.1×10^6 copies mL^{-1}) (Figure S7). At Blind Oso, total bacteria were closely associated with DO ($\rho = 0.72$, $p = 0.008$) (Figure 2.4). Total bacteria at the Gulf were significantly higher ($p = 0.01$) during high dust days and were negatively associated with DOC ($\rho = -0.63$, $p = 0.03$), and positively associated with day of dust AOD ($\rho = 0.74$, $p = 0.006$) and 24hr lag to dust AOD ($\rho = 0.66$, $p = 0.02$) (Figure 2.6).

PCA analysis was conducted to visualize the relationships between the abiotic and biotic variables, and samples were grouped by site. Dim1 explained 41.6% of variation

and Dim2 explained 25.3%. The analysis depicts a distinct clustering by site and to a lesser degree by dust AOD (point size) at both Blind Oso and the Gulf. Both sites exhibited positive associations with a 24 lag to dust. Blind Oso was primary associated with organic and inorganic nutrients, TSS, chlorophyll-*a*, DO, and *V. vulnificus, V. cholerae* while the Gulf had positive associations with culturable *Vibrio* (CFU mL^{-1}) and NH_4^+, while both Blind Oso and the Gulf were associated with the 24 h lag to dust. The Canals had a positive association with both temperature and salinity (Figure 2.8).

Discussion:

Each summer, Saharan dust aerosols carrying nutrients and trace metals, are transported across the Atlantic via easterly trade winds and are deposited in the surface waters of the tropical and subtropical Atlantic, Caribbean, and Gulf of Mexico (Goudie & Middleton, 2001; Lenes et al., 2012). Deposition of dust derived nutrients has the potential to result in compositional shifts in both bacterial and picoeukaryote communities by favoring those that are capable of responding rapidly to the influx of new substrates, nutrients, and trace metals. Among heterotrophic bacteria, this often includes groups that are opportunistic and conditionally rare, such that they can temporarily outcompete other microbes for resources and increase in abundance for short periods, including bacteria that are known to be associated with human illness, such as *Vibrio*. While this relationship has been studied *in situ* in the pelagic and off-shore coastal waters of the Florida Keys, Barbados, and mid-Atlantic (Borchardt et al., 2020; Westrich et al., 2016, 2018), it is currently unknown how comparable the findings are in nearshore coastal and inland regions, where nutrients may be higher, temperature and salinity more variable, and human exposure more likely. As a result of these baseline conditions, the

impacts of dust deposition in these on microbial communities may differ in these environments. This study presents a high-resolution time series that captured a Saharan dust deposition event and its impact on the biology and biogeochemistry in nearshore coastal and inland waters of Corpus Christi, TX.

Dust

Dust AOD levels suggest a dust event was captured during the time series, with light influx occurring on July 13th, and heavy influx on July 16th to July 18th (Figure 2.2). Saharan dust is a significant source of biologically important nutrients including different forms of nitrogen, phosphorous, and iron (Goudie & Middleton, 2001; Graham & Duce, 1982; Mills et al., 2004; Savoie et al., 1989). In this study, significant associations between dust AOD and various forms of nitrogen (NH_4^+, NO_3^- + NO_2^-, DIN, TDN, TN) where observed across the three sites, but no nutrient consistently correlated with dust AOD across all sites, likely due to site-specific parameters. Because aerosol samples were not collected during this study, it can only be speculated that these nutrients may be dust derived. These findings are consistent with previous studies that have identified NH_4^+ and NO_3^- as important contributors (18% and 51% respectively) to the nutrient composition in North African aerosols (Goudie & Middleton, 2001; Swap et al., 1996; Talbot et al., 1986b), and studies that have found elevated DIN levels following addition of dust aerosols (Lagaria et al., 2017; Louis et al., 2015). Alternatively, increased DIN levels could be a result of increased biological processing, as Saharan dust events have been shown to increase rates of nitrogen fixation (Lenes et al., 2008; Mills et al., 2004). In addition, increased inorganic nutrients may suggest bacterial remineralization of initial

responders to dust input. Future work should incorporate a higher temporal resolution and aerosol analysis to fully derive the source of these nutrients.

Biological Response

A notable relationship between initial increases in *Vibrio* abundance 24 h after Saharan dust onset was evident at both Blind Oso and the Gulf. CCA aided in identifying an initial 24 h lag to dust onset (Figure S5), but the lagged trend is not consistent throughout the dust period. Dust influx was continuous and increasing for the latter half of the time series (Figure 2.2), therefore, following initial input, the priming of dust on *Vibrio* abundance may be dynamic, resulting in peaks of in *Vibrio* abundance occurring on different time scales following peaks in dust AOD. A 24 h delay in response is consistent with previous studies documenting an up to 30-fold increase in culturable *Vibrio* in the Florida Keys and Barbados and a 1.5-fold increase in the mid-Atlantic (Westrich et al., 2016, 2018), each occurring 14-24h following dust deposition. This initial temporal delay may be indicative of preliminary processing that occurs in the water column that provides the marine bacterium with more soluble forms of nutrients. It may be that *Vibrio* are responding to the dissolved fraction of dust-derived nutrients as opposed to particulate forms, suggesting that other marine microbes may play an important role in the initial processing of bioavailable dust-derived nutrients.

Although there were some broad responses across the three sites during the times series, specific timing, and degree of increase of *Vibrio* bacteria were highly dependent on local background dynamics including baseline nutrient levels and salinity ranges. Because autotrophic and heterotrophic communities are limited by the same nutrients (e.g., nitrogen, phosphorous) the baseline nutritional status of an environment has the

potential to play an important role in the degree of metabolic response following nutrient input. In low nutrient settings, small-celled bacteria have an advantage in acquiring and utilizing delivered nutrients, and the dominant metabolism is heterotrophic. Conversely, in environments with higher nutrient levels, bacterial populations may be less limited, and competition for inorganic nutrients is alleviated, resulting in a net-autotrophic environment (Marañon et al., 2010). Thus, the underlying nutritional dynamics of these sites may play an important role in dictating microbial response to dust input.

The Loop Current is an important source of water supply to the Gulf of Mexico, as it brings in warm low nutrient waters from the Caribbean Sea to the Gulf, and thus this region is typically characterized as a low nutrient system (Fennel & Laurent, 2018; McKinney et al., 2021; Ward, 2017). The Gulf of Mexico site exhibited significant increases in both total bacteria and total *Vibrio*, with each having significant correlations with dust AOD. Additionally, this site exhbited the greatest degree of increase in *Vibrio* (CFU mL^{-1} and copies mL^{-1}). Here, the westward flux of biologically important nutrients NO_3^- (1.47 Tg yr^{-1}), PO_4^{3-} (0.11 Tg yr^{-1}), and Fe (7.5 Tg yr^{-1}) (Gao et al., 2001; Goudie & Middleton, 2001), may be temporarily releiving this system of nutrient limitation, allowing for significant blooms in responsive bacteria, specifically *Vibrio*. These findings are consistent with previous studies conducted in low nutrient environments that have shown increases heterotrophic bacteria during dust events including Vibrionales, *Pelagibacteracea*, *Rhodobacteriaceae*, *Bacteroidetes*, and Gammaproteobacteria (Borchardt et al., 2020; Guo et al., 2016; Westrich et al., 2016). In this case, it may be that the deposited nutrients are quickly being utilized by rapid responding microbes, and

thus the continuously increasing supply of dust throughout the time series is efficient in supporting increases in bacteria, specifically *Vibrio.*

Blind Oso was highly dynamic and there were likely other variables that coincided with, and confounded dust input that led to a response. This site exhibited comparably higher levels of nutrients (PO_4^{3-}, $NO_3 + NO_2^-$, and TOC) and chlorophyll-*a*, both during the study period (Figure 2.3), and year-round (Manalilkada Sasidharan et al., In Progress; Wetz et al., 2016) (Table S1). Here, the higher levels of nutrients at Blind Oso may be priming the bacterial community, resulting in nutrient influx not having as profound of an impact on *Vibrio* abundance. Additionally, bacterial abundance was order(s) of magnitude greater than the Canals and Gulf (Figure S7), and *Vibrio* were estimated to average < 0.001% of the total bacterial community (Figure S8) indicating that the higher nutrient dynamics of Blind Oso has the potential to support a greater bacterial diversity. While *Vibrio* at Blind Oso exhibited an initial increase in abundance, a plateau was observed during the latter half of the time series despite continued nutrient influx. In this case, the attenuated abundance may be due to the priming of other responders competing for nutrients, or a higher abundance of bacteriophages and protist grazers, dampening what would be an expected more drastic response following increased nutrient influx.

Of particular note, during the latter half of the time series (coinciding with dust influx), Blind Oso exhibited stark changes in salinity, nutrient levels (NO_3+NO_2^-, PO_4^{3-}, TN, TOC), DO, and chlorophyll-*a* (Figure 2.3). Such a sharp decrease in salinity despite the lack of precipitation, in combination with nutrient influx, may be a result of a discharge event from the Oso WWTP. This is further supported by increases in human

fecal marker HF183 concentrations during this timeframe (Figure S3) which has previously been reported at this site (Nicolau & Hill, 2013). In this case, an influx of nutrients from a discharge event may be initially supporting *Vibrio* populations, but ultimately an increase in the autotrophic community prevails, resulting in the observed increase in DO levels during this time frame (Figure 2.3). Additionally, the decrease in salinity at Blind Oso during the latter half of the timeseries (down to 20), in combination with nutrient influx (Figure 2.3) may be driving increases of potentially pathogenic species *V. cholerae* and *V. vulnificus*, as they both typically prefer lower salinities (Takemura et al., 2014). It should be noted that *V. cholerae* at Blind Oso displayed high variability among the 5 technical replicates (Figure 2.7) which may in part be due to methodological limitations and should be interpreted with caution, however the presence of *V. cholerae* at this site warrants further research investigating the specific dynamics of this species at this site. It is likely that at Blind Oso, nutrient influx in combination with decreasing salinity is what resulted in increases in *Vibrio* (and potentially pathogenic species), however the degree of influence of dust deposition cannot be fully determined, as heavy dust days coincided with a potential WWTP discharge event. It can be hypothesized that these events then may have a potentially synergistic or independent role in driving *Vibrio* dynamics, but more work is needed to elucidate this matter.

No clear correlation between dust and *Vibrio* abundance was observed at the Canals. This may in part be due to the consistently high salinity at this site during the time series (Figure 2.3). With the exception of some *Vibrio* species (*V. cholerae, V. mimicus, V. vulnificus*), *Vibrio* generally prefer brackish and marine waters. Salinity extremes (both high and low) have the potential to foster an environment that is

inhospitable for the growth of most *Vibrio* species. Additionally, there may also be a higher abundance of grazers or bacteriophages at this site that are exerting a top-down control on *Vibrio* abundances.

Ecological and Health Implications

Blooms of *Vibrio* and specific species that are known to be pathogenic towards humans can result in a higher risk of exposure to the public. In tandem with rising sea surface temperatures, *Vibrio* cases in humans have been increasing globally and expanding geographically with cases being detected as far north as Alaska and ~100 miles from the Arctic circle. (Baker-Austin et al., 2016; Froelich & Daines, 2020; McLaughlin et al., 2005; Newton et al., 2012; World Health Organization, 2016). Further, surveillance data indicates *Vibrio* related illnesses have more than doubled in the U.S since 1997 (CDC, 2023; Newton et al., 2012). In Texas alone, cases have been increasing steadily since 1988 with waterborne infections (e.g. swimming) beginning to outpace foodborne infections (CDC, 2018). Outside of the well-studied role of temperature (and to some degree salinity) in promoting *Vibrio* growth and increasing exposure risk, few predictable environmental parameters exist that can be used to reliably predict favorable conditions for growth and exposure risk. Dust deposition may be able to serve as a predictor, but more work is needed to understand this. With a heightened risk of *Vibrio* exposure in coastal waters, it is vital that we expand upon our understanding of microbial dynamics following dust input, and of how the degree of response may vary depending on location-specific environmental parameters. The findings from this study provide new insight on the conditions that can elicit potentially harmful bacterial blooms in nearshore coastal and inland environments.

Conclusion:

This study effectively captured blooms of bacteria, particularly *Vibrio* (including potentially pathogenic species *V. cholerae* and *V. vulnificus*), with the promotion (and differences in degree) of the blooms most likely being driven by site-specific dynamics. These findings suggest that inland sites such as Blind Oso, are highly dynamics, and there are likely multiple factors cooccurring that may drive *Vibrio* abundance. Whereas, low nutrient coastal sites may be experiencing a temporary relief from nutrient limitation as Saharan dust deposits biologically important nutrients, resulting in significant blooms of the marine bacterium *Vibrio*. This opens a line of questions that aim to address the specific ecological and biogeochemical mechanisms that are driving increases in abundance in these inland and coastal regions. Anthropogenic induced climate change is driving increases in global ocean temperatures and with this comes a heightened risk of *Vibrio* exposure (Froelich & Daines, 2020). Additionally, climatic driven droughts have the potential to increase dust storm frequency in some areas (Akhtar, 2020; Held et al., 2005). Combined, there is a potential to see increased *Vibrio* blooms in response to dust input, and a higher risk to public health in coastal and inland waters, where human interaction is common. Together these findings provide a unique insight into the specific conditions that elicit blooms of potentially harmful bacteria in nearshore coastal waters.

Acknowledgements:

Funding for this work was included a grant from Texas SeaGrant to EKL (NA18OAR4170088 -> M2200767-02-417011-00037)

References:

Akhtar, R. (Ed.). (2020). *Extreme Weather Events and Human Health: International Case Studies*. Springer International Publishing. https://doi.org/10.1007/978-3-030-23773-8

American Public Health Association; Citation: APHA (2005) Standard Methods for the Examination of Water and Wastewater. *21st Edition*.

Baker-Austin, C., Oliver, J. D., Alam, M., Ali, A., Waldor, M. K., Qadri, F., & Martinez-Urtaza, J. (2018). Vibrio spp. Infections. *Nature Reviews Disease Primers*, *4*(1), 1–19. https://doi.org/10.1038/s41572-018-0005-8

Baker-Austin, C., Trinanes, J. A., Salmenlinna, S., Löfdahl, M., Siitonen, A., Taylor, N. G. H., & Martinez-Urtaza, J. (2016). Heat Wave–Associated Vibriosis, Sweden and Finland, 2014. *Emerging Infectious Diseases*, *22*(7), 1216–1220. https://doi.org/10.3201/eid2207.151996

Ben-Haim, Y., Thompson, F. L., Thompson, C. C., Cnockaert, M. C., Hoste, B., Swings, J., & Rosenberg, E. (2003). Vibrio coralliilyticus sp. Nov., a temperature-dependent pathogen of the coral Pocillopora damicornis. *International Journal of Systematic and Evolutionary Microbiology*, *53*(1), 309–315. https://doi.org/10.1099/ijs.0.02402-0

Borchardt, T., Fisher, K. V., Ebling, A. M., Westrich, J. R., Xian, P., Holmes, C. D., Landing, W. M., Lipp, E. K., Wetz, M. S., & Ottesen, E. A. (2020). Saharan dust

deposition initiates successional patterns among marine microbes in the Western Atlantic. *Limnology and Oceanography*, *65*(1), 191–203. https://doi.org/10.1002/lno.11291

Bustin, S. A., Benes, V., Garson, J. A., Hellemans, J., Huggett, J., Kubista, M., Mueller, R., Nolan, T., Pfaffl, M. W., Shipley, G. L., Vandesompele, J., & Wittwer, C. T. (2009). The MIQE Guidelines: Minimum Information for Publication of Quantitative Real-Time PCR Experiments. *Clinical Chemistry*, *55*(4), 611–622. https://doi.org/10.1373/clinchem.2008.112797

CDC. (2019). *Vibrio species causing Vibriosis*. https://www.cdc.gov/vibrio/faq.html

CDC. (2023). *Pathogen Surveillance*. Centers for Disease Control and Prevention. https://www.cdc.gov/FoodNetFast

Fennel, K., & Laurent, A. (2018). N and P as ultimate and proximate limiting nutrients in the northern Gulf of Mexico: Implications for hypoxia reduction strategies. *Biogeosciences*, *15*(10), 3121–3131. https://doi.org/10.5194/bg-15-3121-2018

Formenti, P. (2003). Chemical composition of mineral dust aerosol during the Saharan Dust Experiment (SHADE) airborne campaign in the Cape Verde region, September 2000. *Journal of Geophysical Research*, *108*(D18), 8576. https://doi.org/10.1029/2002JD002648

Froelich, B. A., & Daines, D. A. (2020). In hot water: Effects of climate change on *Vibrio* –human interactions. *Environmental Microbiology*, *22*(10), 4101–4111. https://doi.org/10.1111/1462-2920.14967

Gao, Y., Kaufman, Y. J., Tanré, D., Kolber, D., & Falkowski, P. G. (2001). Seasonal distributions of aeolian iron fluxes to the global ocean. *Geophysical Research Letters*, *28*(1), 29–32. https://doi.org/10.1029/2000GL011926

Goudie, A. S., & Middleton, N. J. (2001). Saharan dust storms: Nature and consequences. *Earth-Science Reviews*, *56*(1), 179–204. https://doi.org/10.1016/S0012-8252(01)00067-8

Graham, W. F., & Duce, R. A. (1982). The atmospheric transport of phosphorus to the western North Atlantic. *Atmospheric Environment (1967)*, *16*(5), 1089–1097. https://doi.org/10.1016/0004-6981(82)90198-6

Greenfield, D. I., Gooch Moore, J., Stewart, J. R., Hilborn, E. D., George, B. J., Li, Q., Dickerson, J., Keppler, C. K., & Sandifer, P. A. (2017). Temporal and Environmental Factors Driving Vibrio Vulnificus and V. Parahaemolyticus Populations and Their Associations With Harmful Algal Blooms in South Carolina Detention Ponds and Receiving Tidal Creeks. *GeoHealth*, *1*(9), 306–317. https://doi.org/10.1002/2017GH000094

Griffin, D. W., Garrison, V. H., Herman, J. R., & Shinn, E. A. (2001). *African desert dust in the Caribbean atmosphere: Microbiology and public health*.

Guo, C., Xia, X., Pitta, P., Herut, B., Rahav, E., Berman-Frank, I., Giannakourou, A., Tsiola, A., Tsagaraki, T. M., & Liu, H. (2016). Shifts in Microbial Community Structure and Activity in the Ultra-Oligotrophic Eastern Mediterranean Sea Driven by the Deposition of Saharan Dust and European Aerosols. *Frontiers in Marine Science*, *3*. https://www.frontiersin.org/articles/10.3389/fmars.2016.00170

Harrell, F. E. (2023). *Hmisc: Harrell Miscellaneous* (R package version 5.1-0) [Computer software]. https://CRAN.R-project.org/package=Hmisc

Hayes, K. (2020). *A Eutrophic Assessment of Two South Texas Estuaries*. Texas A&M University-Corpus Christi.

Held, I. M., Delworth, T. L., Lu, J., Findell, K. L., & Knutson, T. R. (2005). Simulation of Sahel drought in the 20th and 21st centuries. *Proceedings of the National Academy of Sciences*, *102*(50), 17891–17896. https://doi.org/10.1073/pnas.0509057102

Herut, B., Zohary, T., Krom, M. D., Mantoura, R. F. C., Pitta, P., Psarra, S., Rassoulzadegan, F., Tanaka, T., & Frede Thingstad, T. (2005). Response of East Mediterranean surface water to Saharan dust: On-board microcosm experiment and field observations. *Deep Sea Research Part II: Topical Studies in Oceanography*, *52*(22), 3024–3040. https://doi.org/10.1016/j.dsr2.2005.09.003

Ina-Salwany, M. Y., Al-saari, N., Mohamad, A., Mursidi, F.-A., Mohd-Aris, A., Amal, M. N. A., Kasai, H., Mino, S., Sawabe, T., & Zamri-Saad, M. (2019). Vibriosis in Fish: A Review on Disease Development and Prevention. *Journal of Aquatic Animal Health*, *31*(1), 3–22. https://doi.org/10.1002/aah.10045

Jones, J. (2022). *Standard Operating Procedures for: Real-time PCR for Total VP, Pathogenic Vp, and Vv for the National Shellfish Sanitation Program (NSSP)*.

Kassambara, A., & Mundt, F. (2020). *factoextra: Extract and Visualize the Results of Multivariate Data Analyses* (R package version 1.0.7) [Computer software]. https://CRAN.R-project.org/package=factoextra

Kellogg, C. A., Griffin, D. W., Garrison, V. H., Peak, K. K., Royall, N., Smith, R. R., & Shinn, E. A. (2004). Characterization of Aerosolized Bacteria and Fungi From Desert Dust Events in Mali, West Africa. *Aerobiologia*, *20*(2), 99–110. https://doi.org/10.1023/B:AERO.0000032947.88335.bb

Lagaria, A., Mandalakis, M., Mara, P., Papageorgiou, N., Pitta, P., Tsiola, A., Kagiorgi, M., & Psarra, S. (2017). Phytoplankton Response to Saharan Dust Depositions in the Eastern Mediterranean Sea: A Mesocosm Study. *Frontiers in Marine Science*, *3*. https://www.frontiersin.org/articles/10.3389/fmars.2016.00287

Laghdass, M., Blain, S., Besseling, M., Catala, P., Guieu, C., & Obernosterer, I. (2011). Effects of Saharan dust on the microbial community during a large in situ mesocosm experiment in the NW Mediterranean Sea. *Aquatic Microbial Ecology*, *62*(2), 201–213. https://doi.org/10.3354/ame01466

Lê, S., Jusso, J., & Husson, F. (2008). *FactoMineR: A Package for Multivariate Analysis*. *25*(1), 1–18. https://doi.org/10.18637/jss.v025.i01

Lekunberri, I., Lefort, T., Romero, E., Vázquez-Domínguez, E., Romera-Castillo, C., Marrasé, C., Peters, F., Weinbauer, M., & Gasol, J. M. (2010). Effects of a dust deposition event on coastal marine microbial abundance and activity, bacterial community structure and ecosystem function. *Journal of Plankton Research*, *32*(4), 381–396. https://doi.org/10.1093/plankt/fbp137

Lenes, J. M., Darrow, B. A., Walsh, J. J., Prospero, J. M., He, R., Weisberg, R. H., Vargo, G. A., & Heil, C. A. (2008). Saharan dust and phosphatic fidelity: A three-dimensional biogeochemical model of Trichodesmium as a nutrient source for red

tides on the West Florida Shelf. *Continental Shelf Research*, *28*(9), 1091–1115. https://doi.org/10.1016/j.csr.2008.02.009

Lenes, J. M., Prospero, J. M., Landing, W. M., Virmani, J. I., & Walsh, J. J. (2012). A model of Saharan dust deposition to the eastern Gulf of Mexico. *Marine Chemistry*, *134–135*, 1–9. https://doi.org/10.1016/j.marchem.2012.02.007

Louis, J., Bressac, M., Pedrotti, M. L., & Guieu, C. (2015). Dissolved inorganic nitrogen and phosphorus dynamics in seawater following an artificial Saharan dust deposition event. *Frontiers in Marine Science*, *2*. https://doi.org/10.3389/fmars.2015.00027

Lynch, P., Reid, J. S., Westphal, D. L., Zhang, J., Hogan, T. F., Hyer, E. J., Curtis, C. A., Hegg, D. A., Shi, Y., Campbell, J. R., Rubin, J. I., Sessions, W. R., Turk, F. J., & Walker, A. L. (2016). An 11-year global gridded aerosol optical thickness reanalysis (v1.0) for atmospheric and climate sciences. *Geoscientific Model Development*, *9*(4), 1489–1522. https://doi.org/10.5194/gmd-9-1489-2016

Manalilkada Sasidharan et al., (In Progress).

Marañon, E., Fernández, A., Mouriño-Carballido, B., MartÍnez-GarcÍa, S., Teira, E., Cermeño, P., Chouciño, P., Huete-Ortega, M., Fernández, E., Calvo-DÍaz, A., Morán, X. A. G., Bode, A., Moreno-Ostos, E., Varela, M. M., Patey, M. D., & Achterberg, E. P. (2010). Degree of oligotrophy controls the response of microbial plankton to Saharan dust. *Limnology and Oceanography*, *55*(6), 2339–2352. https://doi.org/10.4319/lo.2010.55.6.2339

McKinney, L. D., Shepherd, J. G., Wilson, C. A., Hogarth, W. T., Chanton, J., Murawski, S. A., Sandifer, P. A., Sutton, T., Yoskowitz, D., Wowk, K., Özgökmen, T. M., Joye, S. B., & Caffey, R. (2021). *The Gulf of Mexico AN OVERVIEW*.

McLaughlin, J. B., DePaola, A., Bopp, C. A., Martinek, K. A., Napolilli, N. P., Allison, C. G., Murray, S. L., Thompson, E. C., Bird, M. M., & Middaugh, J. P. (2005). Outbreak of Vibrio parahaemolyticus Gastroenteritis Associated with Alaskan Oysters. *New England Journal of Medicine*, *353*(14), 1463–1470. https://doi.org/10.1056/NEJMoa051594

Merkes, C. M., Klymus, K. E., Allison, M., Goldberg, C. S., Helbin, C., Hunter, M. E., Jackson, C. A., Lance, R., Mangan, A., Monroe, E. M., Piagio, A., Stokdyk, J. P., Wilson, C., & Richter, C. A. (2019). *Reporting the limits of detection (LOD) and quantification (LOQ) for environmental DNA assays: Data* [dataset]. U.S. Geological Survey. https://doi.org/10.5066/P9AKHU1R

Mills, M. M., Ridame, C., Davey, M., La Roche, J., & Geider, R. J. (2004). Iron and phosphorus co-limit nitrogen fixation in the eastern tropical North Atlantic. *Nature*, *429*(6989), 292–294. https://doi.org/10.1038/nature02550

Newton, A., Kendall, M., Vugia, D. J., Henao, O. L., & Mahon, B. E. (2012). Increasing Rates of Vibriosis in the United States, 1996–2010: Review of Surveillance Data From 2 Systems. *Clinical Infectious Diseases*, *54*(suppl_5), S391–S395. https://doi.org/10.1093/cid/cis243

Nicolau, B., & Hill, E. (2013). *Support for Total Maximum Daily Loads (TMDL) for Indicator Bacteria in Oso Bay Interim Monitoring Report Fiscal Year 2013*

(Year-one). https://www.tceq.texas.gov/downloads/water-quality/tmdl/oso-bay-oyster-harvesting-assessment-103/103-oso-bay-monitoring-report-2013.pdf

Norfolk, W. A. (2023). *VIBRIO ALGINOLYTICUS: A PHYSIOLOGICAL, CHEMICAL, AND ECOLOGICAL CHARACTERIZATION OF AN EMERGING MARINE PATHOGEN*.

Pruzzo, C., Vezzulli, L., & Colwell, R. R. (2008). Global impact of Vibrio cholerae interactions with chitin. *Environmental Microbiology*, *10*(6), 1400–1410. https://doi.org/10.1111/j.1462-2920.2007.01559.x

R Core Team. (2022). *R: A language and environment for statistical computing.* [Computer software]. URL https://www.R-project.org/)

R Studio Team. (2022). *RStudio: Integrated Development Environment for R*. http://www.rstudio.com/

Ramírez-Camejo, L. A., Zuluaga-Montero, A., Morris, V., Rodríguez, J. A., Lázaro-Escudero, M. T., & Bayman, P. (2022). Fungal diversity in Sahara dust: Aspergillus sydowii and other opportunistic pathogens. *Aerobiologia*, *38*(3), 367–378. https://doi.org/10.1007/s10453-022-09752-9

Randa, M. A., Polz, M. F., & Lim, E. (2004). Effects of Temperature and Salinity on Vibrio vulnificus Population Dynamics as Assessed by Quantitative PCR. *Applied and Environmental Microbiology*, *70*(9), 5469–5476. https://doi.org/10.1128/AEM.70.9.5469-5476.2004

Reche, I., Ortega-Retuerta, E., Romera, O., Villena, E. P., Baquero, R. M., & Casamayor, E. O. (2009). Effect of Saharan dust inputs on bacterial activity and community

composition in Mediterranean lakes and reservoirs. *Limnology and Oceanography*, *54*(3), 869–879. https://doi.org/10.4319/lo.2009.54.3.0869

Richards, G. P., Watson, M. A., Needleman, D. S., Church, K. M., & Häse, C. C. (2015). Mortalities of Eastern and Pacific Oyster Larvae Caused by the Pathogens Vibrio coralliilyticus and Vibrio tubiashii. *Applied and Environmental Microbiology*, *81*(1), 292–297. https://doi.org/10.1128/AEM.02930-14

Savoie, D. L., Prospero, J. M., & Saltzman, E. S. (1989). Non-sea-salt sulfate and nitrate in trade wind aerosols at Barbados: Evidence for long-range transport. *Journal of Geophysical Research*, *94*(D4), 5069. https://doi.org/10.1029/JD094iD04p05069

Shade, A., Jones, S. E., Caporaso, J. G., Handelsman, J., Knight, R., Fierer, N., & Gilbert, J. A. (2014). Conditionally Rare Taxa Disproportionately Contribute to Temporal Changes in Microbial Diversity. *mBio*, *5*(4), 10.1128/mbio.01371-14. https://doi.org/10.1128/mbio.01371-14

Sodders, N., Stockdale, K., Baker, K., Ghanem, A., Vieth, B., & Harder, T. (2023). Notes from the Field: Vibriosis Cases Associated with Flood Waters During and After Hurricane Ian — Florida, September–October 2022. *Morbidity and Mortality Weekly Report*, *72*(18), 497–498. https://doi.org/10.15585/mmwr.mm7218a5

Stein, A., Draxler, R., Rolph, G., Stunder, B., Cohen, M., & Ngan, F. (2015). *NOAA's HYSPLIT atmospheric transport and dispersion modeling system*. *96*(12), 2059–2077.

Swap, R., Ulanski, S., Cobbett, M., & Garstang, M. (1996). Temporal and spatial characteristics of Saharan dust outbreaks. *Journal of Geophysical Research: Atmospheres*, *101*(D2), 4205–4220. https://doi.org/10.1029/95JD03236

Takemura, A., Chien, D., & Polz, M. (2014). Associations and dynamics of Vibrionaceae in the environment, from the genus to the population level. *Frontiers in Microbiology*, *5*. https://www.frontiersin.org/articles/10.3389/fmicb.2014.00038

Talbot, R. W., Harriss, R. C., Browell, E. V., Gregory, G. L., Sebacher, D. I., & Beck, S. M. (1986). Distribution and geochemistry of aerosols in the tropical north Atlantic troposphere: Relationship to Saharan dust. *Journal of Geophysical Research*, *91*(D4), 5173. https://doi.org/10.1029/JD091iD04p05173

Texas Commission on Environmental Quality. (2022). *2022 Integrated Report—Texas 303(d) List (Category 5)*.

Thompson, J. R., Randa, M. A., Marcelino, L. A., Tomita-Mitchell, A., Lim, E., & Polz, M. F. (2004). Diversity and Dynamics of a North Atlantic Coastal Vibrio Community. *Applied and Environmental Microbiology*, *70*(7), 4103–4110. https://doi.org/10.1128/AEM.70.7.4103-4110.2004

Tran, L., Nunan, L., Redman, R., Mohney, L., Pantoja, C., Fitzsimmons, K., & Lightner, D. (2013). Determination of the infectious nature of the agent of acute hepatopancreatic necrosis syndrome affecting penaeid shrimp. *Diseases of Aquatic Organisms*, *105*(1), 45–55. https://doi.org/10.3354/dao02621

Turner, J. W., Good, B., Cole, D., & Lipp, E. K. (2009). Plankton composition and environmental factors contribute to Vibrio seasonality. *The ISME Journal*, *3*(9), Article 9. https://doi.org/10.1038/ismej.2009.50

Ushijima, B., Meyer, J. L., Thompson, S., Pitts, K., Marusich, M. F., Tittl, J., Weatherup, E., Reu, J., Wetzell, R., Aeby, G. S., Häse, C. C., & Paul, V. J. (2020). Disease Diagnostics and Potential Coinfections by Vibrio coralliilyticus During an

Ongoing Coral Disease Outbreak in Florida. *Frontiers in Microbiology*, *11*. https://www.frontiersin.org/articles/10.3389/fmicb.2020.569354

Walker, L. M., Montagna, P. A., Hu, X., & Wetz, M. S. (2020). Timescales and Magnitude of Water Quality Change in Three Texas Estuaries Induced by Passage of Hurricane Harvey. *Estuaries and Coasts*, *44*(4), 960–971. https://doi.org/10.1007/s12237-020-00846-6

Ward, C. H. (2017). Habitats and biota of the Gulf of Mexico: Before the deepwater horizon oil spill. In *Habitats and Biota of the Gulf of Mexico: Before the Deepwater Horizon Oil Spill* (p. 868). https://doi.org/10.1007/978-1-4939-3447-8

Wei, T., & Simko, V. (2021). *R package "corrplot": Visualization of a Correlation Matrix* (Version 0.92) [Computer software]. https://github.com/taiyun/corrplot

Westrich, J. R., Ebling, A. M., Landing, W. M., Joyner, J. L., Kemp, K. M., Griffin, D. W., & Lipp, E. K. (2016). Saharan dust nutrients promote *Vibrio* bloom formation in marine surface waters. *Proceedings of the National Academy of Sciences*, *113*(21), 5964–5969. https://doi.org/10.1073/pnas.1518080113

Westrich, J. R., Griffin, D. W., Westphal, D. L., & Lipp, E. K. (2018). Vibrio Population Dynamics in Mid-Atlantic Surface Waters during Saharan Dust Events. *Frontiers in Marine Science*, *5*, 12. https://doi.org/10.3389/fmars.2018.00012

Wetz, M. S. (n.d.). *Publication CBBEP - 114 Project Number – 1312 June 2014*.

Wetz, M. S., Cira, E. K., Sterba-Boatwright, B., Montagna, P. A., Palmer, T. A., & Hayes, K. C. (2017). Exceptionally high organic nitrogen concentrations in a semi-arid South Texas estuary susceptible to brown tide blooms. *Estuarine, Coastal and Shelf Science*, *188*, 27–37. https://doi.org/10.1016/j.ecss.2017.02.001

Wetz, M. S., Hayes, K. C., Fisher, K. V. B., Price, L., & Sterba-Boatwright, B. (2016). Water quality dynamics in an urbanizing subtropical estuary(Oso Bay, Texas). *Marine Pollution Bulletin*, *104*(1–2), 44–53. https://doi.org/10.1016/j.marpolbul.2016.02.013

Wickham, H. (2016). *ggplot2: Elegant Graphics for Data Analysis*. Springer-Verlag New York. https://ggplot2.tidyverse.org

World Health Organization. (2016). *Cholera – Global situation*. https://www.who.int/emergencies/disease-outbreak-news/item/2022-DON426

Figures:

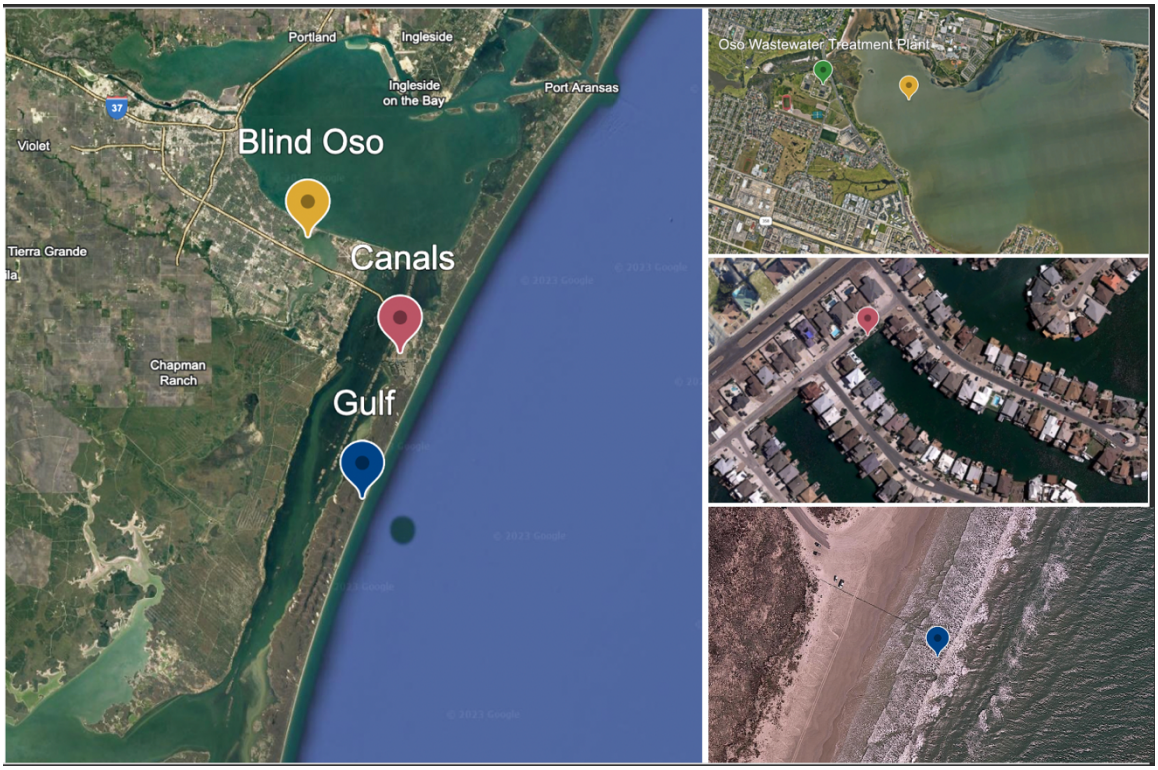

Figure 2.1: Sample collection locations by site: Blind Oso Bay (yellow), Residential Canals (pink), Gulf of Mexico (blue) (Google Earth).

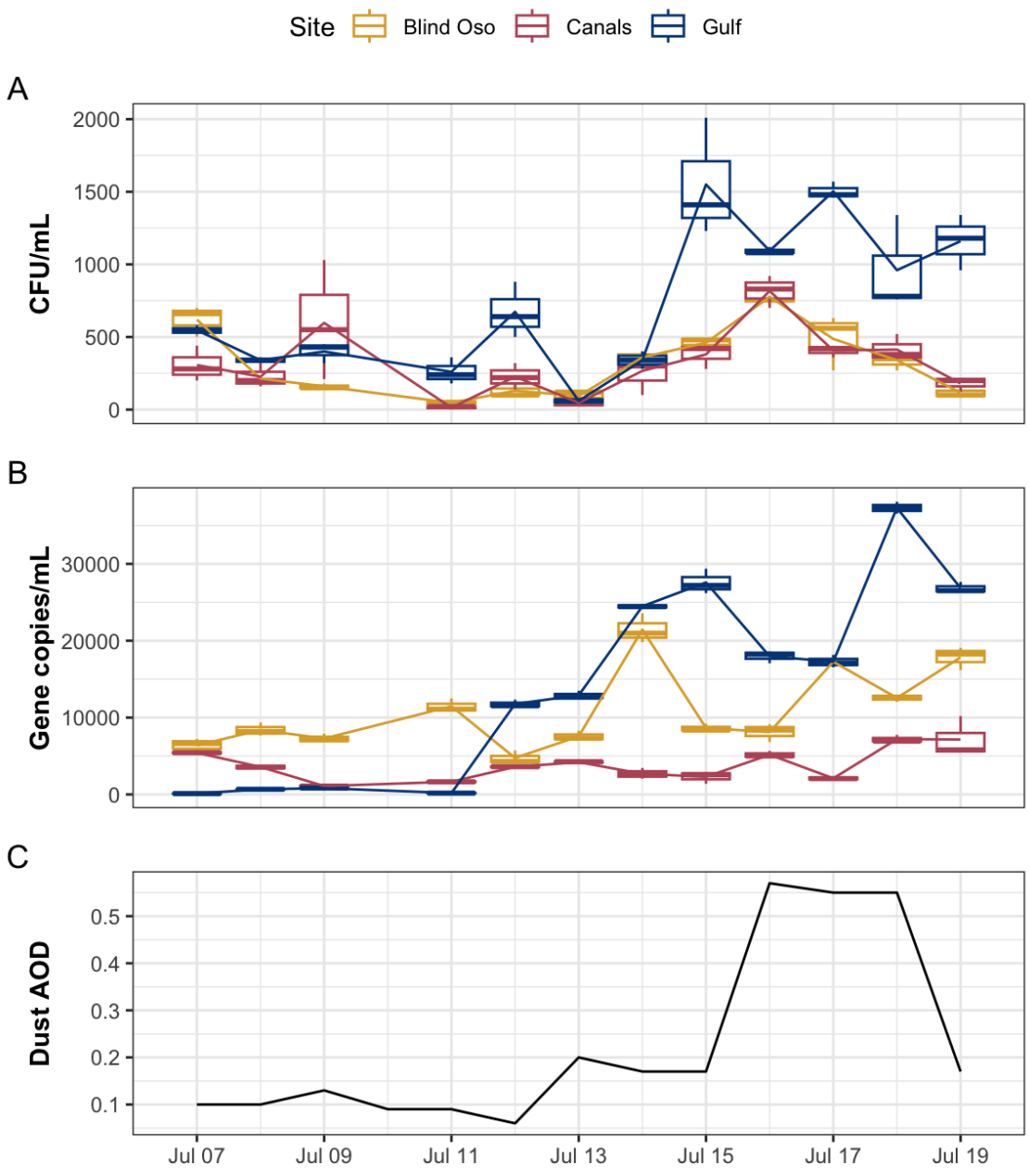

Figure 2.2: Total *Vibrio* enumerated as CFU mL^{-1} (A) and copies mL^{-1} (B), and dust AOD (C) across the daily time series by site: Blind Oso (yellow), Canals (pink), Gulf (blue). Boxplots represent technical triplicates of culture and qPCR data, and dust was calculated as a 24h composite sum of the 6 h collection intervals prior to time of collection (7:00 am Central Daylight Time).

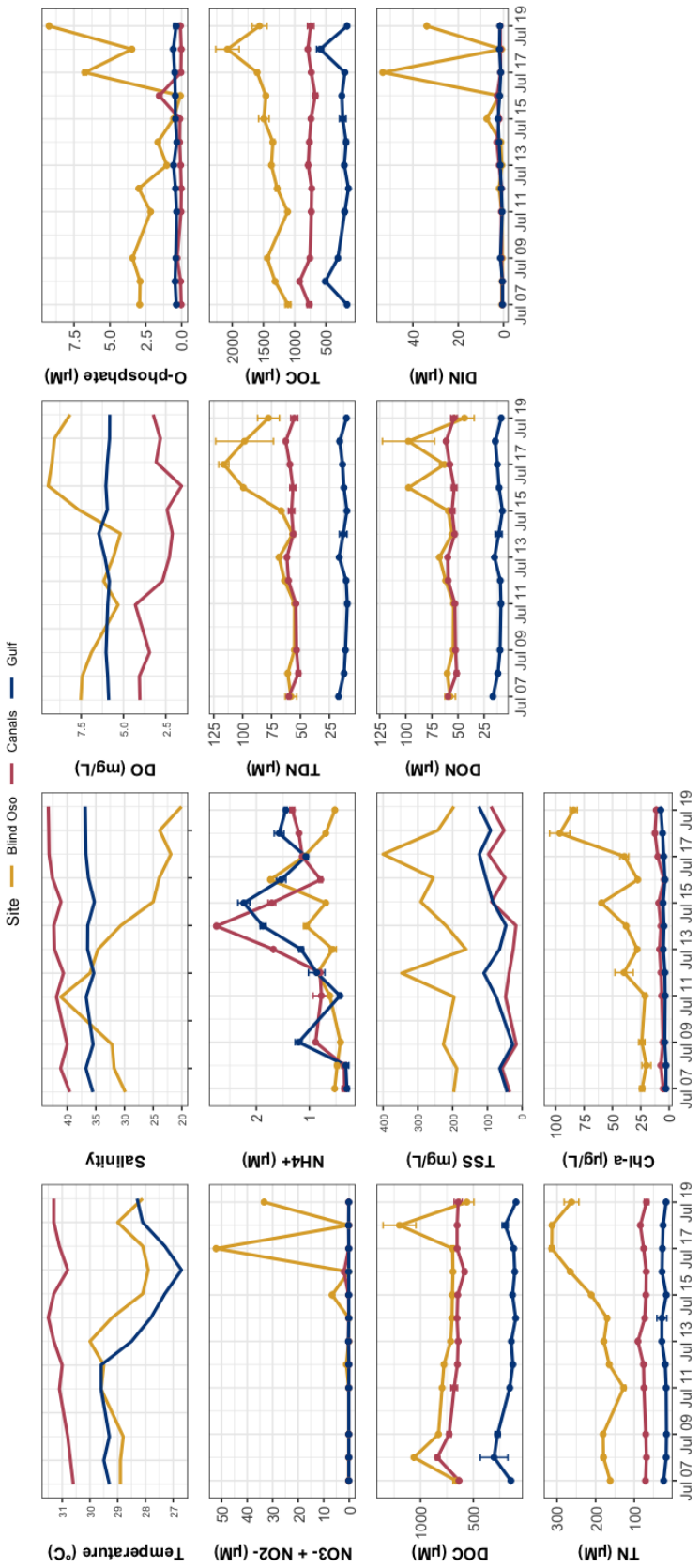

Figure 2.3: Water quality parameters collected during time series by site: Blind Oso (yellow), Canals (pink), Gulf (blue).

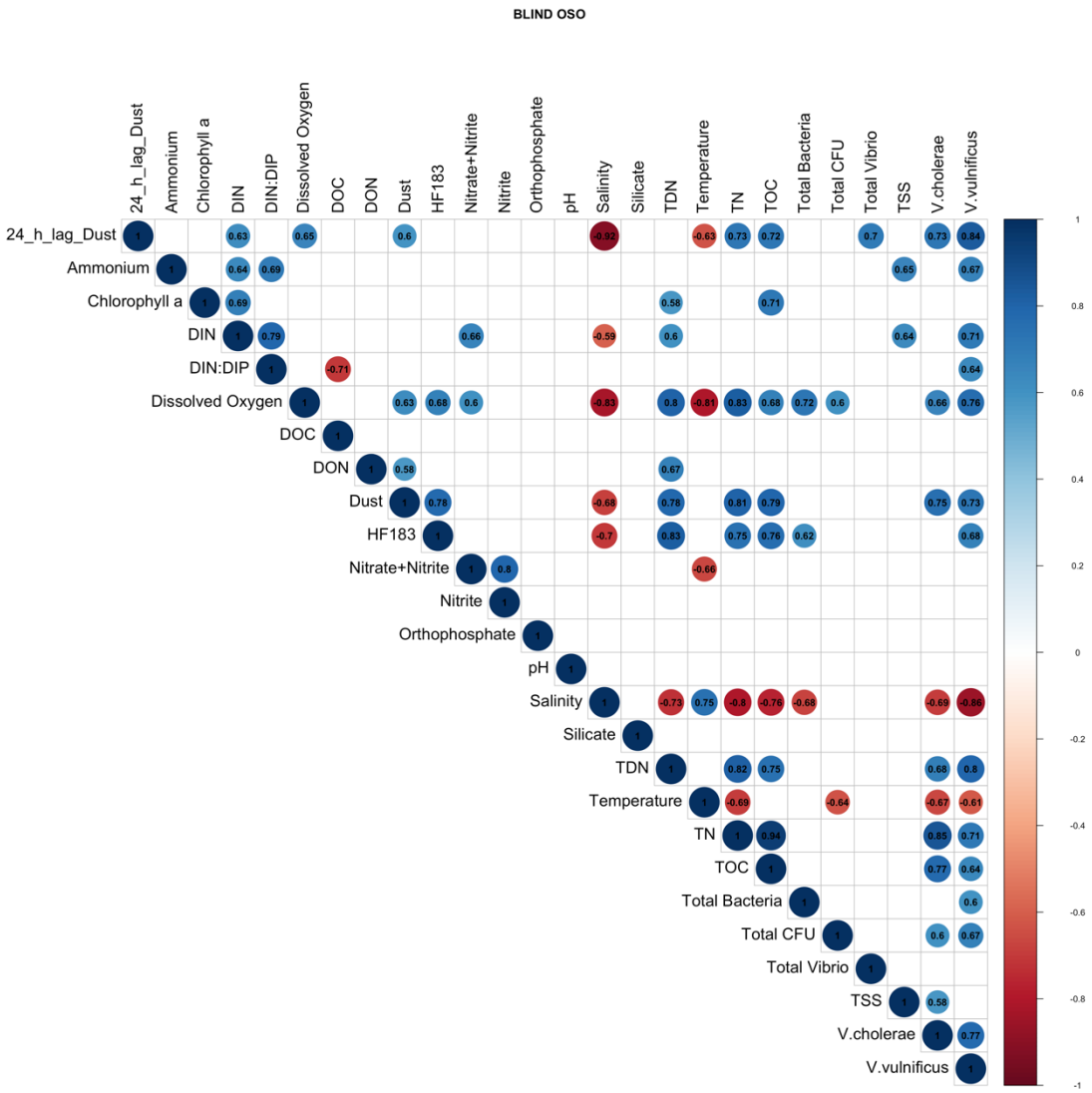

Figure 2.4: Spearman's Correlation heatmap of Blind Oso.

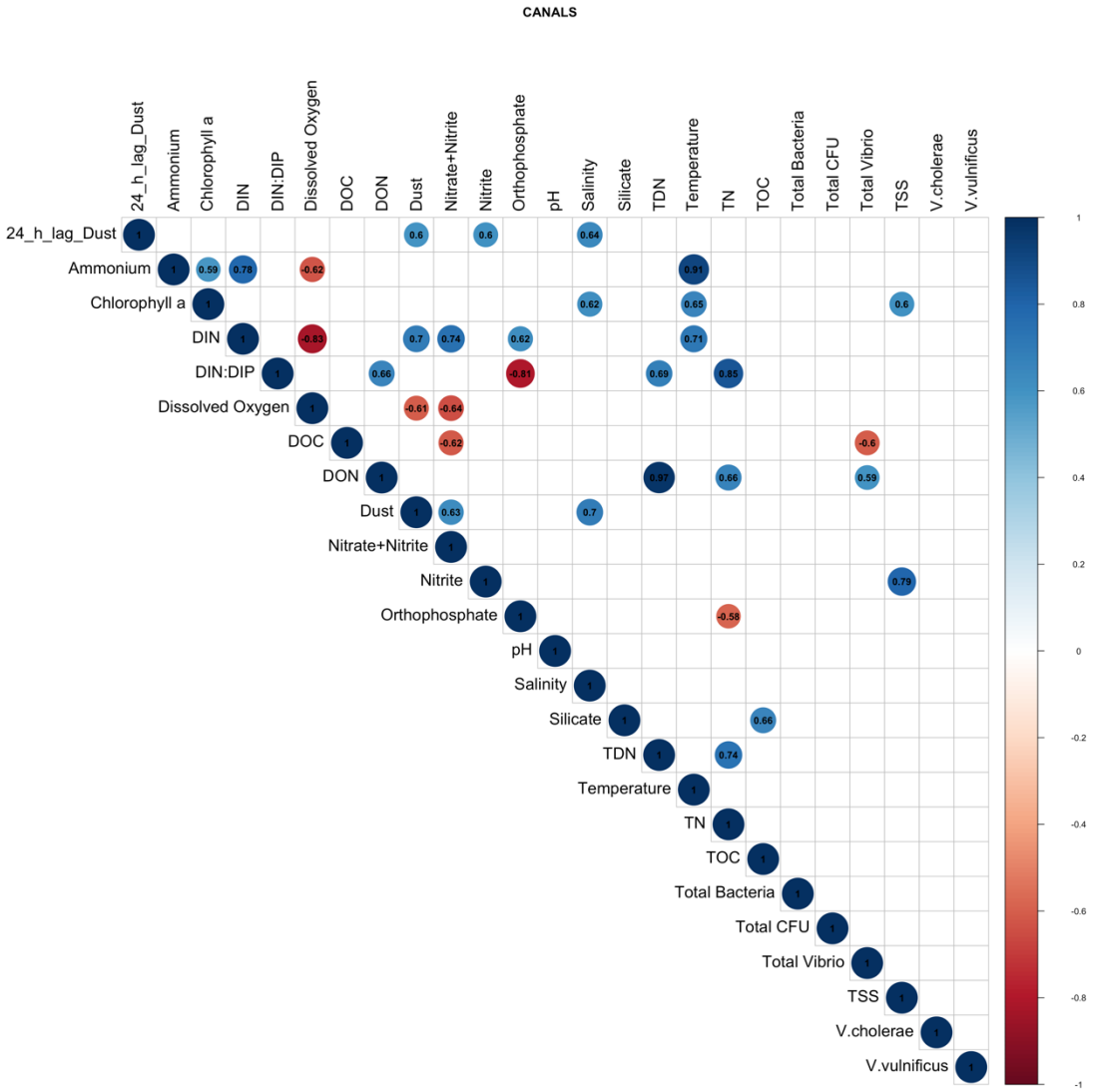

Figure 2.5: Spearman's Correlation heatmap of the Canals.

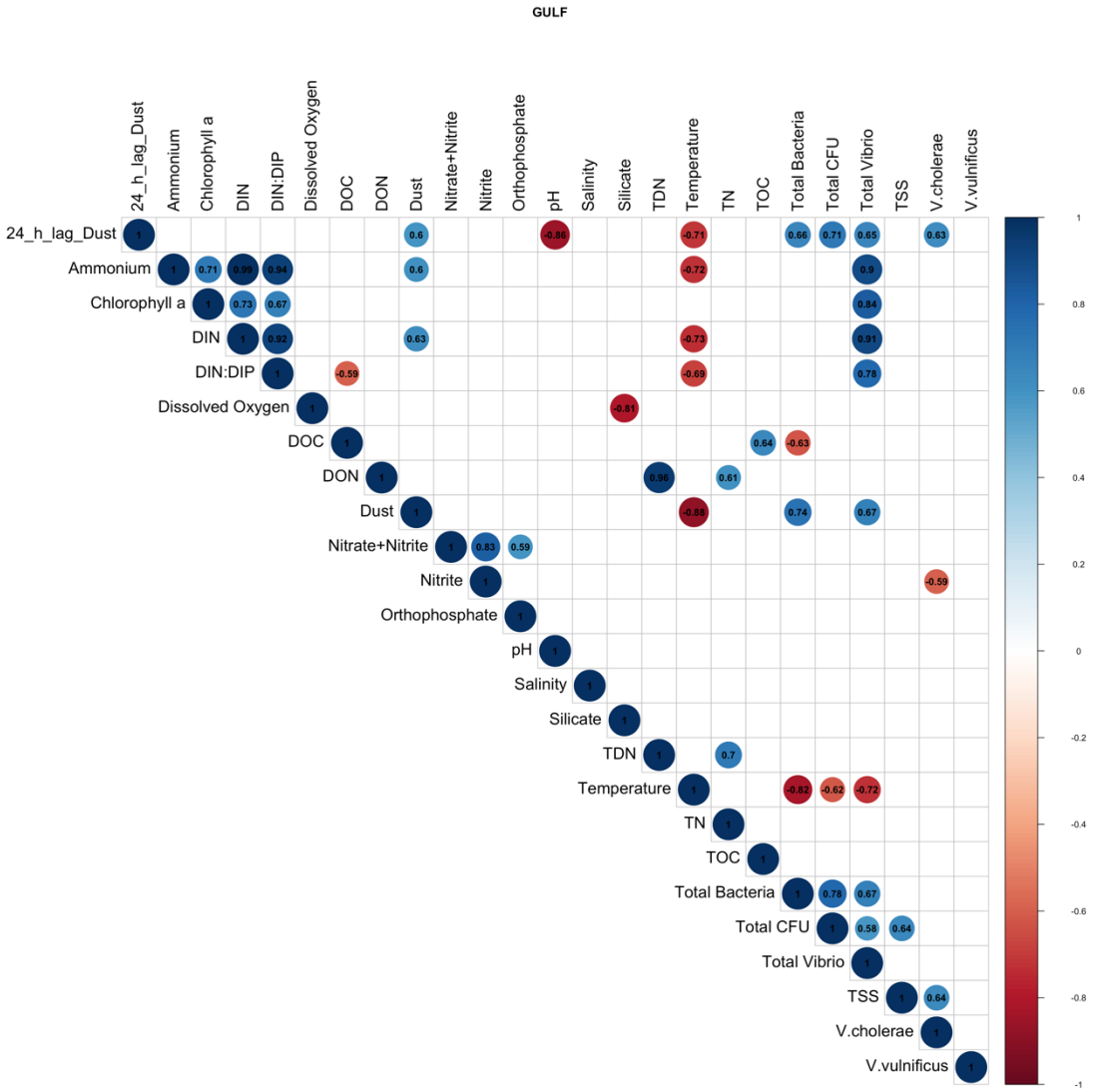

Figure 2.6: Spearman's Correlation heatmap of the Gulf.

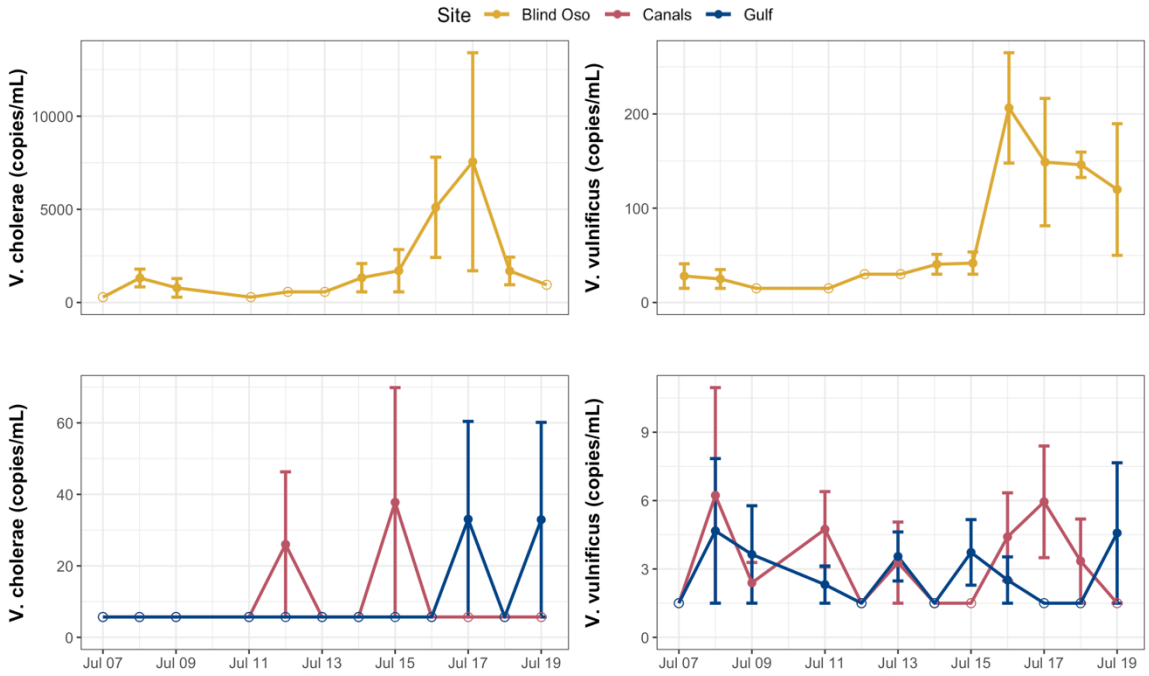

Figure 2.7: *Vibrio* species concentrations (copies mL^{-1}) across the daily time series by site: Blind Oso (yellow), Canals (pink), Gulf (blue). Open circles indicate that all replicates were below the detection limit. Sites that had all points below detection limit were omitted from the figure. Bars represent standard error of the technical replicates.

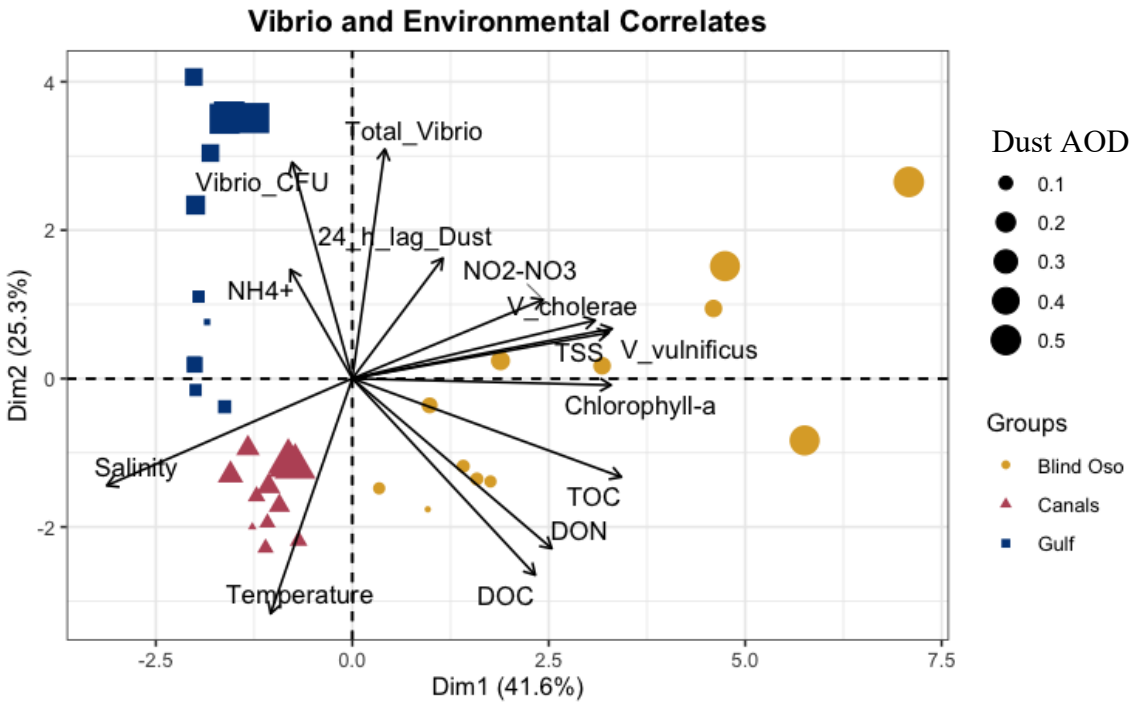

Figure 2.8: PCA Analysis during high frequency time series showing distinct clustering by site (color) and to a lesser degree by dust AOD (point size).

CHAPTER 3

CONCLUSION

Each summer, episodic plumes of Saharan dust travel across the Atlantic to be deposited in the surface waters of the Caribbean and Gulf of Mexico. Dust aerosols have been shown to serve as a significant source of nutrients (nitrate, phosphate, iron) that can potentially facilitate the development of microbial blooms (including *Vibrio*) in offshore and pelagic environments. However, the potential effect of deposition events in more dynamic inland coastal waters is not well understood. This study aimed to quantify *Vibrio* population dynamics and composition in response to dust events in regions where environmental parameters are more variable, and human risk of exposure is higher. This study effectively captured blooms of bacteria, particularly *Vibrio* (including pathogenic species *V. cholerae* and *V. vulnificus*), with increases in abundance likely being driven by site-specific dynamics. During dust days, total *Vibrio* concentrations increased significantly at two of the three sites ($p < 0.05$), with greatest increase noted at the Gulf of Mexico site. Following dust deposition, *Vibrio* abundance at the Gulf may be exhibiting drastic increases as a result of temporary relief from nutrient limitation. The dampened but significant increase at Blind Oso on the other hand may have been due to synergistic nutrient loadings from both dust deposition and WWTP discharge, but more work is needed to fully elucidate the cause of increased abundances here. This opens up a line of questions that aim to address the specific ecological, biological, and

physiochemical mechanisms that are driving increases in abundance in these inland and nearshore regions. Anthropogenic induced climate change is driving increases in global ocean temperatures and with this comes a heightened risk of *Vibrio* exposure. With the exception of temperature, and to some degree salinity, few predictors exist that can accurately assess risk of exposure. Saharan dust influx may be able to serve as a predictor, but more work is needed. The findings from this study serve as a foundational baseline, providing new insight on the conditions that can elicit potentially harmful bacterial blooms in nearshore coastal and inland environments.

APPENDIX

Tables:

Table S1: Monthly Water Quality Data

Date	Site	Salinity	Temperature (°C)	PO_4^{3-} (µM)	NO3+NO2$^-$ (µM)	NH_4^+ (µM)	Depth (m)
2022-02-16	Gulf	NA	NA	NA	NA	NA	NA
2022-03-09	Gulf	28.66	13.5	0.35	0.24	0.32	0.5
2022-04-20	Gulf	30.94	23.5	0.3	0.14	1.05	0.5
2022-05-11	Gulf	30.88	27	0.1	0.12	0.24	0.6
2022-06-14	Gulf	34.65	27.5	0.21	0.15	0.39	0.5
2022-07-18	Gulf	36.79	28.1	0.58	0.24	1.57	0.5
2022-08-09	Gulf	37.25	29.9	0.52	0.14	1.19	0.5
2022-09-13	Gulf	36.67	29.6	0.46	0.06	1.49	1.5
2022-10-18	Gulf	30.02	23.3	0.85	0.51	2.5	0.6
2022-11-15	Gulf	31.31	18.7	0.7	0.42	2.4	0.4
2022-12-14	Gulf	31.91	19.4	0.62	0.83	2.91	0.5
2022-02-16	Canals	29.12	16.3	0.12	0.19	0.38	1.2
2022-03-09	Canals	29.4	16	0.3	1.56	2.33	1.3
2022-04-20	Canals	32.46	25.1	0.4	1.23	2.28	1.5
2022-05-11	Canals	35.46	29.1	0.06	0.26	0.35	1.4
2022-06-14	Canals	37.7	30.3	0.05	0.11	0.76	1.3
2022-07-18	Canals	43.2	31.3	0.02	0.17	1.2	1.3
2022-08-09	Canals	45.55	31	0.05	0.14	1.33	1.4
2022-09-13	Canals	37.29	30.6	0.4	1.48	7.01	1.6
2022-10-18	Canals	36.9	25.7	0.91	1.68	13.22	1.7
2022-11-15	Canals	34.3	19.3	0.82	3.52	7.72	1.6
2022-12-14	Canals	32.8	22.4	0.23	0.47	2.1	1.6
2022-02-16	Blind Oso	23.88	19.9	12.16	62.27	7.6	0.5
2022-03-09	Blind Oso	29.06	12.7	2.25	7.11	5.44	0.6
2022-04-20	Blind Oso	31.58	24.1	0.73	0.39	3.67	1
2022-05-11	Blind Oso	32.18	28.3	1.21	0.23	0.57	0.6
2022-06-14	Blind Oso	30.41	27.8	5.61	14.06	9.66	0.5
2022-07-18	Blind Oso	23.87	29	3.47	0.17	0.69	0.4
2022-08-09	Blind Oso	37.06	29.6	4.95	0.17	1.29	0.7
2022-09-13	Blind Oso	28.73	30.8	4.92	6.78	1.75	0.7
2022-10-18	Blind Oso	32.65	18.8	10.44	35.55	19.28	0.9
2022-11-15	Blind Oso	31.16	15.7	5.42	29.42	2.64	0.8
2022-12-14	Blind Oso	31.99	20.5	2.09	7.41	2.68	0.8

Table S2: Primer, Probe, and Standard sequences used for qPCR

Target Gene	Primer and Probe Sequences (5'-3')	Standards (G-Blocks)	Reference
Total *Vibrio* (*16S rRNA*) (SYBR)	567F: GGCGTAAAGCGCATGCAGGT 680R: GAAATTCTACCCCCCTCTACAG	CGAATTCTCTCATTTAGGACGGCGTAAA GCGCATGCAGGTCCTAGTAAGTCATCATT GGTATTTGAATGCGACCCCGAAGAAACC GCCTAAAAATGTCAATGGTTGGTCCACT GTAGAGGGGGGTAGAATTTCCTAAACTT CATTTAATC	Westrich et al., 2018
V. alginolyticus (*gyrB*) (SYBR)	gyrBF: ATTGAGAACCCGACAGAAGCGAAG gyrBR: CCTAATGCGGTGATCAGTGTTACT	TCTTGATTGAGAACCCGACAGAAGCGAA GATGGTTTGTTCGAAAATCATCAATGCA GCACGTGCATCTGAAGCAGCGCCTAAAG CTCGTGAAATGACGCGCCGTAAAGGTGC ACTAGACCTAGCAGGCCTTCCAGGTAAA GTTGCAGACTGTCAGGAAAAAGATCCGG CACTCTTTGAACTATACATAGTGGAGGGT GAATCGGCAGGCGGTTCCGCAAAACAAG GCCGTAACCGTAAGAACCAAGCGATCAC ACCGCTAAAAGGTAAGATTCTTAACGTA GAAAAAGCACGTTTCGACAAGATGCTAT CTTCTCTAGAAGTAGTAACACTGATCACC GCATTAGGTTGTG	Zhou et al., 2007
V. cholerae (*lolB*) (SYBR)	VC195F:CCGTTGAGGCGAGTTTGGTGAGA VC195R: GTGCGCGGGTCGAAACTTATGAT	GTGCTGAACTTACAGGTCGATGAACAAG GTGCGCGGGTCGAAACTTATGAGATCAA ATCTACCGCGACCAAGATGCACAAAGCC TGATCCGCAATTTAACAGGGTTAGATATT CCCGTTGAACAGCTTGAAGATTGGATTTT AGGCTTGCCGACCCAAGCAACCCATTAC GAGTTGAATGAACAAAACACCCTTGCCA CTCTCACCAAACTCGCCTCAACGGCCGA ATGGCACGTGGAATACCAACGTTA	Cho, 2013
V. vulnificus (*vvh*) (Taqman)	vvhF: TGTTTATGGTGAGAACGGTGACA vvhR: TTCTTTATCTAGGCCCCAAACTTG vvh Probe: HEX™/ZEN™-CCGTTAACCGAACCACCCGCAA- IB®FQ	ATGAGTCACTGAGCAACAACGATCTCTG CCTAGATGTTTATGGTGAGAACGGTGAC AAAACGGTTGCGGGTGGTTCGGTTAACG GCTGGAGCTGTCACGGCAGTTGGAACCA AGTTTGGGGCCTAGATAAAGAAGAACGT TACCGTAGCCGAGTAGCATCCGATCGTT GTTTGACCGTAAACGCAGACAAAACGCT CACAGTCGAACAGTGTGGTGCGAACTTA GCACAGAAATGGTATTGGGAAATTAG	Jones, 2022
V. parahaemolyticus (*tlh*) (Taqman)	tlhF: ACTCAACACAAGAAGAGATCGACCA tlhR: GATGAGCGGTTGATGTCCAA tlh Probe: HEX™/ZEN™-CGCTCGCGTTCACGAAACCGT- IB®FQ	ACGACGAAAGCGCCTCAGTTTAAGTACT CAACACAAGAAGAGATCGACAAAATTCG TGCGAAAGTGCTTGAGATGAACGAGTTC ATCAAGGCACAAGCGATGTACTACAAAG CGCAAGGTTACAACATCACGTTGTTTGAT ACTCACGCCTTGTTCGAGACGCTAACTTC TGCGCCAGAAGAGCACGGTTTCGTGAAC GCGAGCGATCCTTGTTTGGACATCAACC GCTCATCGTCTGTCGATTACATGT	Jones, 2022
IAC (Taqman)	IAC 46F: GACATCGATATGGGTGCCG IAC 186R: CGAGACGATGCAGCCATTC IAC Probe: Cy5™ - TCTCATGCGTCTCCCTGGTGAATGTG-BHQ®-2'	NA	Jones, 2022
Total Bacteria (*16S rRNA*) (SYBR)	967F: CAACGCGAAGAACCTTACC 1046R: CGACAGCCATGCANCACT	TACGGCCGCAAGGTTAAAACCAAATGAA TTGACGGGGGCCCGCACAAGCGGTGGAG CATGTGGTTTAATTCGATGCAACGCGAA GAACCTTACCTACTCTTGACATCCAGAGA ACTTTCCAGAGATGGATTGGTGCCTTCGG GAACTCTGAGACAGGTGCTGCATGGCTG TCGTCAGCTCGTGTTGTGAAATGTTGGGT TAAGTCCCGCAACGAGCGCAACCCTTAT CCTTTGTTGCCAGCGGTTAGGC	Sogin et al., 2006
Bacteroides (*HF183*) (Taqman)	HF183F: ATCATGAGTTCACATGTCCG HF183/Bac287R:ATCATGAGTTCACATGTCC GCATGATTAAAGGTATTTTCCGGTAGACG ATGTGTAGCAACGGCGTGTTATAGTAGGC GGGGTAACGGCCCACCTAGTCAACGATGG ATAGGGGTTCTGAGAGGAAG HF183 Probe: 56-FAM-CTGAGAGGAAGGTCCCCCACATTGGA-36-TAMSp	GAAGATTAATCCAGGATGGGATCATGAG TTCACATGTCCGCATGATTAAAGGTATTT TCCGGTAGACGATGGGGATGCGTTCCAT TAGATAGTAGGCGGGGTAACGGCCCACC TAGTCAACGATGGATAGGGGTTCTGAGA GGAAGGTCCCCCACATTGGAACTGAGAC ACGGTCCAAACTCCTACGGGAGGCAGCA GTGAGGAAT	Green et al., 2014

Table S3: Specifications for qPCR Reactions for all targets

Target/Reaction Volume	Reaction Component	Final Concentration
Total *Vibrio* (10µL)	SYBR PowerUp PCR Mastermix	1 X
	Forward/Reverse Primers	0.16 µM
	DNA Template (2.5 µL)	--
V. alginolyticus (15 µL)	SYBR PowerUp PCR Mastermix	1 X
	Forward/Reverse Primers	0.16 µM
	DNA Template (1.2 µL)	--
V. cholerae (15 µL)	SYBR PowerUp PCR Mastermix	1 X
	Forward/Reverse Primers	0.5 µM
	DNA Template (1.5 µL)	--
V. parahaemolyticus/*V. vulnificus* (15 µL)	Platinum Taq	1.12 U
	Forward/Reverse Primers	0.3 µM
	IAC Forward/Reverse Primers	0.08 µM
	Target Probe	0.2 µM
	IAC Probe	0.15 µM
	$MgCL_2$	5 µM
	PCR Buffer	1 X
	dNTPs	0.3 µM
	DNA Template (1.2 µL)	--
Total Bacteria (10 µL)	SYBR PowerUp PCR Mastermix	1 X
	Forward/Reverse Primers	0.2 µM
	DNA Template (2.5 µL)	--
HF183 (20 µL)	TaqPath	1 U
	Forward/Reverse Primers	0.2 µM
	Target Probe	0.1 µM
	DNA Template (5 µL)	--

Table S4: Cycling Parameters used for qPCR

Target Gene	Step	Temperature (°C)	Time (s)	Cycles	Ref.
Total *Vibrio* (16S rRNA)	UDG Activation	50	120	--	(Westrich et al., 2018)
(SYBR)	Taq Activation:	95	120	--	--
	Denaturation:	95	15	x45	--
	Annealing/Extension	60	60		--
V. alginolyticus (gyrB)	Initial Denaturation	95	60	--	(Zhou et al., 2007)
(SYBR)	Denaturation	95	15	x45	--
	Annealing	57*	15		--
	Extension	72	45		--
V. cholerae (lolB)	Initial Denaturation	93	180	--	(Cho, 2013)
(SYBR)	Denaturation: 95°C	95	19	x45	--
	Annealing/Extension	57	20		--
V. vulnificus (vvh)	Initial Denaturation	96	60	--	(Jones, 2022)
(Taqman)	Denaturation	95	5	x45	--
	Annealing	59	45		--
	Extension	72	25		--
V. parahaemolyticus (tlh)	Initial Denaturation	95	60	--	(Jones, 2022)
(Taqman)	Denaturation	95	5	x45	--
	Annealing/Extension	59	45		--
Total Bacteria (16S rRNA)	UDG Activation	50	120	--	(Lydon et al., 2017)
(SYBR)	Initial Denaturation	95	120	--	--
	Denaturation	95	15	x40	--
	Annealing	61	15		--
	Extension	72	60		--
Bacteroides (HF183)	UP Activation: 95°C;10min	95	600	--	(Green et al., 2014)
(Taqman)	Denaturation: 95°C;15sec	95	15	x40	--
	Annealing/Extension	60	60		--

*Altered from original protocol

Figures:

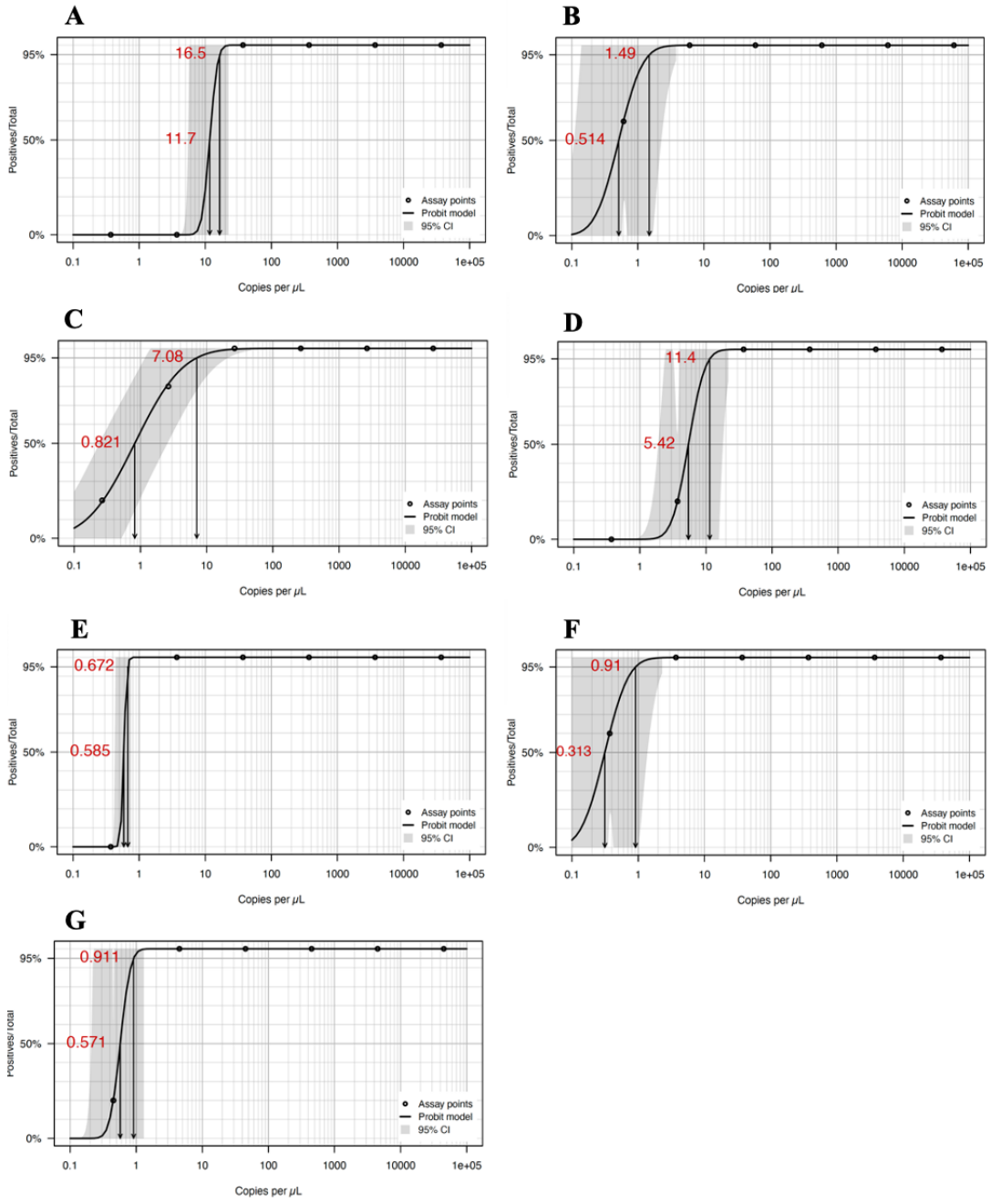

Figure S1: Limit of detection (LOD) probit models for (A) total bacteria, (B) total *Vibrio*, (C) *V. alginolyticus*, (D) *V. cholerae*, (E) *V. parahaemolyticus*, (F) *V. vulnificus*, (G) HF183. Values in red indicate the effective dose of template that was required to achieve a given probability (95% and 50%) of observing a positive qPCR assay.

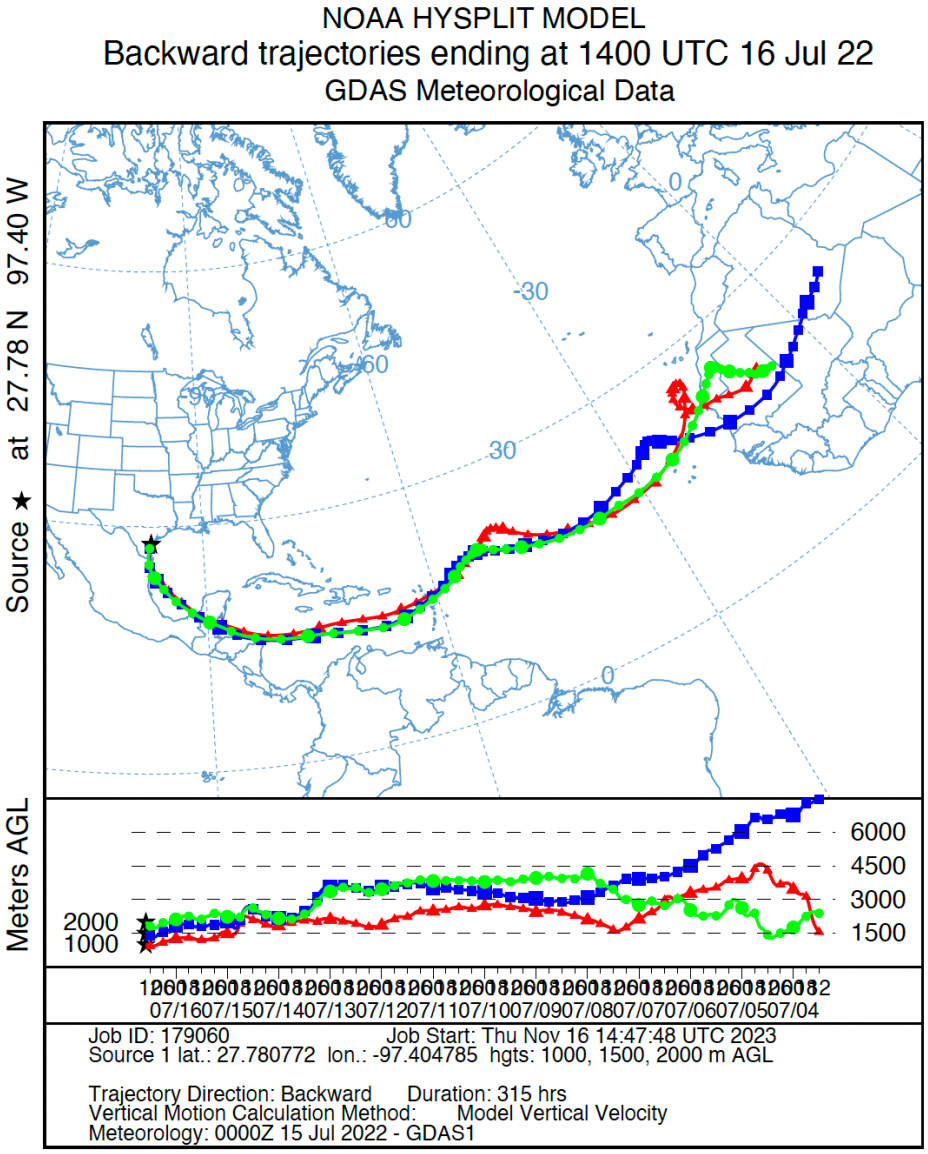

Figure S2: NOAA HYSPLIT backtrack trajectory showing Saharan dust arriving in Corpus Christi, TX on July 16th, 2022. The dust is sourced from the Saharan Desert, and the model began on July 4th, 2022.

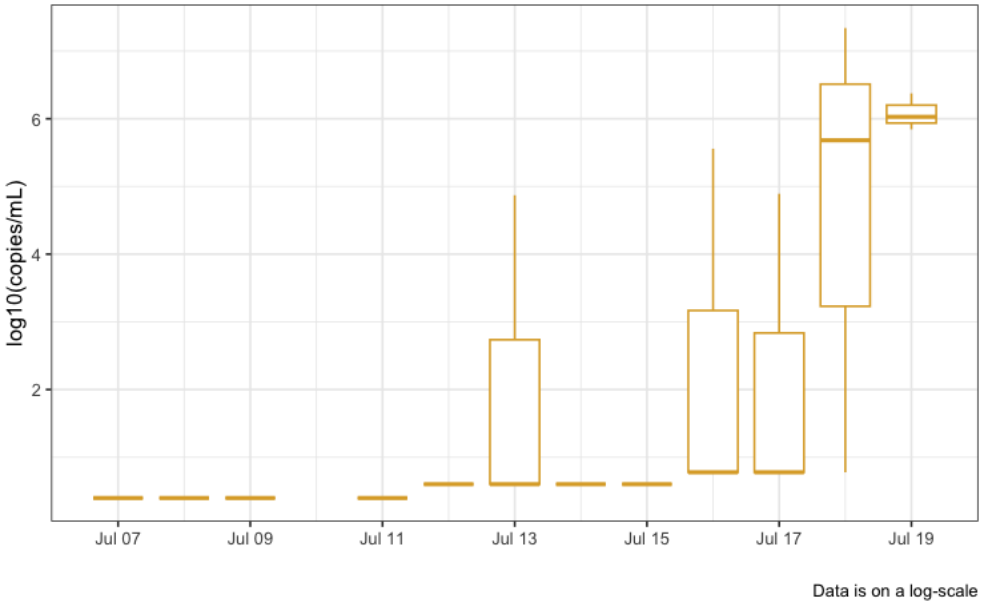

Figure S3: HF183 Levels at Blind Oso during time series. Data is on a log scale.

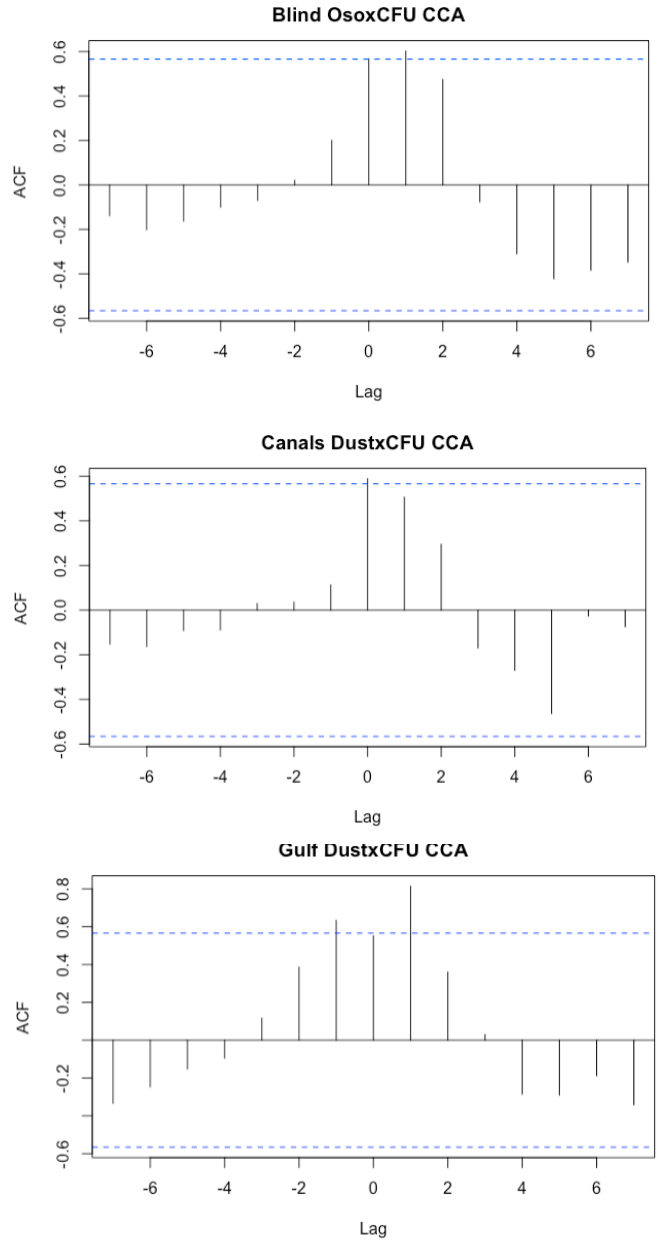

Figure S4: Cross correlation analysis between dust AOD and culturable *Vibrio* (CFU mL^{-1}). A negative Lag value indicates that dust AOD is a predictor of total *Vibrio*. A positive autocorrelation function (ACF) indicates a positive relationship between the two variables. Blue lines indicate 95% confidence interval.

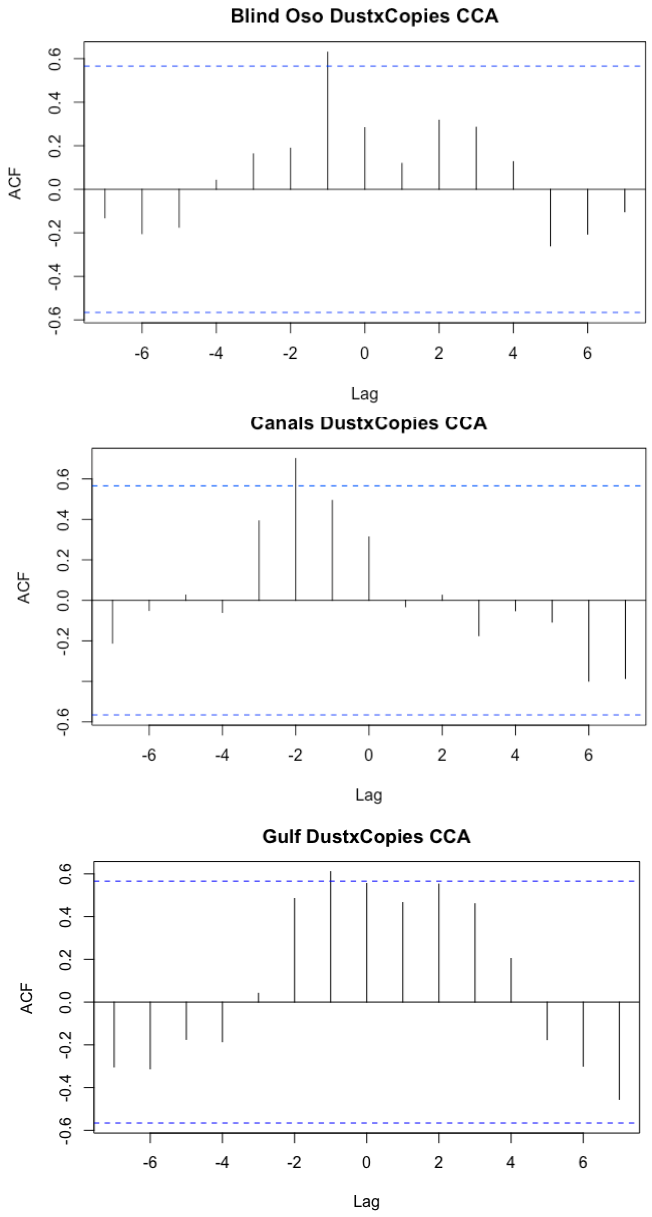

Figure S5: Cross correlation analysis between dust AOD and total *Vibrio* (copies mL^{-1}). A negative Lag value indicates that dust AOD is a predictor of total *Vibrio*. A positive autocorrelation function (ACF) indicates a positive relationship between the two variables. Blue lines indicate 95% confidence interval.

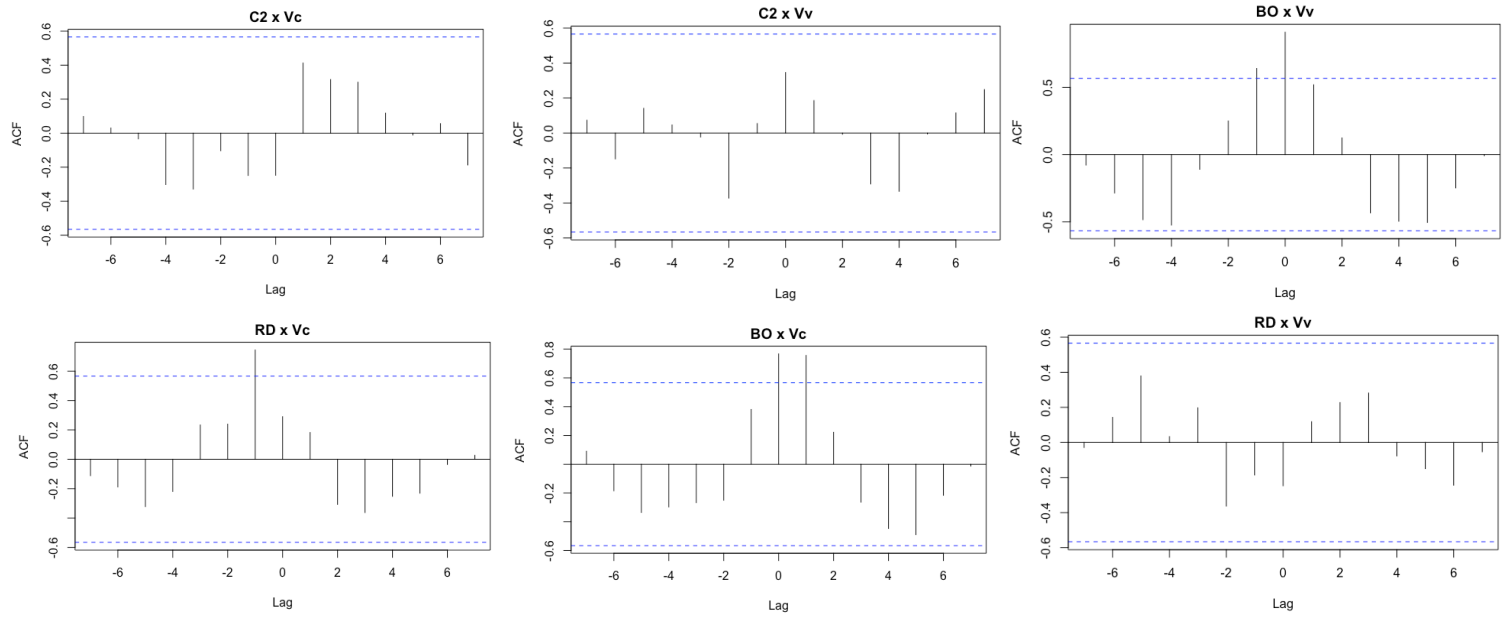

Figure S6: Cross correlation analysis between dust AOD and *Vibrio* species: *V. cholerae* and *V. vulnificus* (copies mL^{-1}). A negative Lag value indicates that dust AOD is a predictor of total *Vibrio*. A positive autocorrelation function (ACF) indicates a positive relationship between the two variables. Blue lines indicate 95% confidence interval.

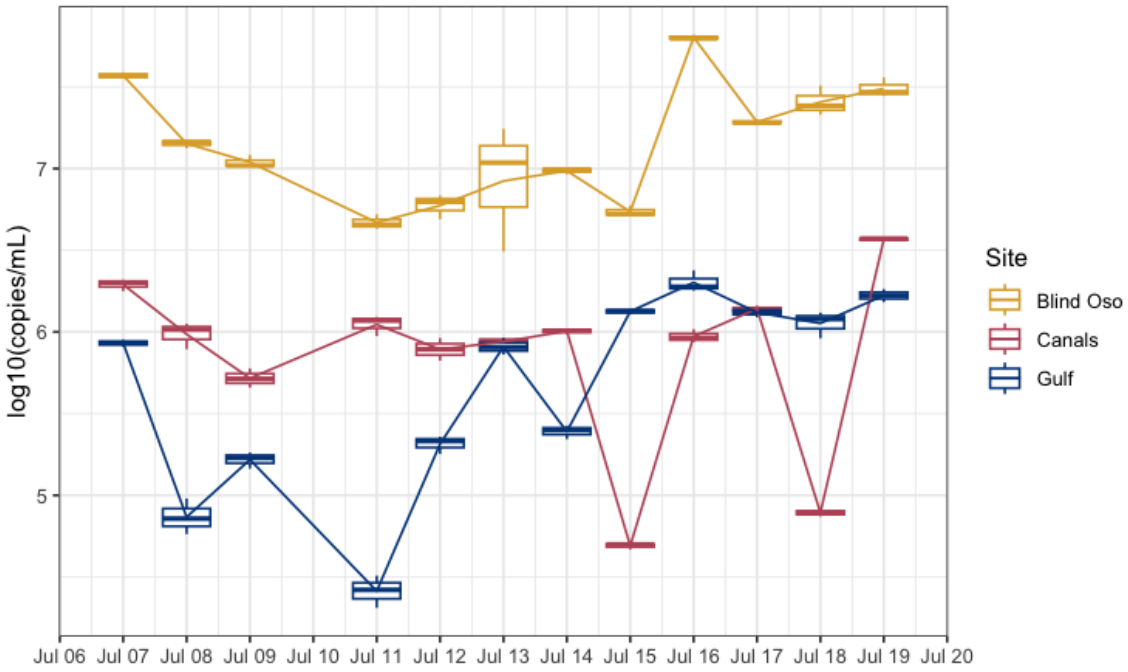

Figure S7: Total bacteria levels (copies mL^{-1}) during daily time series. Data is on a log-scale and color indicates site: Blind Oso (yellow), Canals (pink), Gulf (blue).

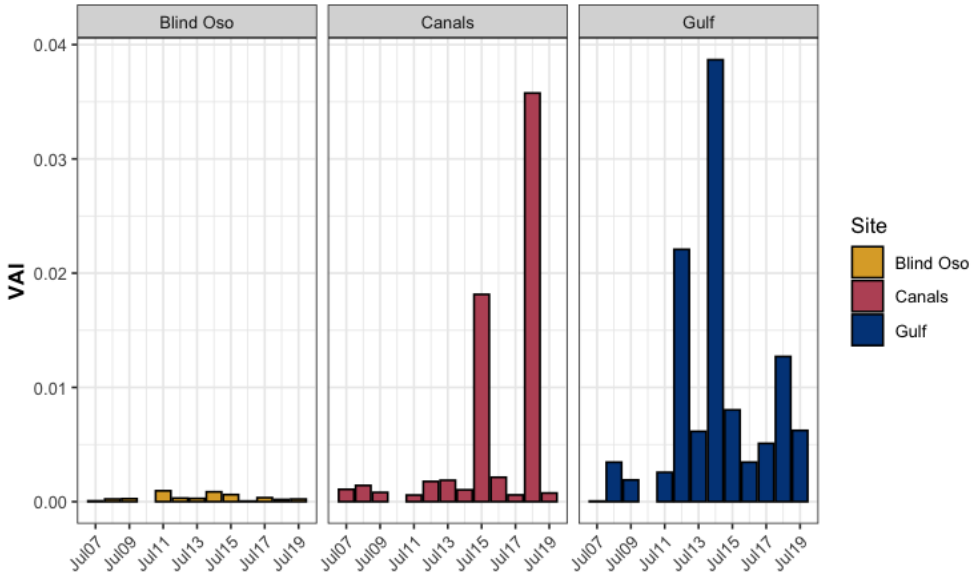

Figure S8: To determine the proportion of *Vibrio* that make up the bacterial community, total *Vibrio* and Bacteria were expressed as cell equivalents (CE) mL^{-1} by dividing the sample 16S rRNA copies mL^{-1} by the average 16s rRNA copy numbers in *Vibrio* (n = 9) and Bacteria (n = 3.5). *Vibrio* Abundance Index (VAI) was determined by taking the proportion of *Vibrio* CE mL^{-1} over the bacterial CE mL^{-1} (Vezzulli et al., 2012). Color indicates site: Blind Oso (yellow), Canals (pink), Gulf (blue).